

RESEARCH ARTICLE

Arctic phytoplankton microdiversity across the marginal ice zone: Subspecies vulnerability to sea-ice loss

Catherine G erikas Ribeiro^{1,*} , Adriana Lopes dos Santos² , Nicole Trefault¹ , Dominique Marie³, Connie Lovejoy⁴ , and Daniel Vaultot^{2,3} 

Seasonal phytoplankton blooms are important Arctic phenomena, contributing to global primary production and biogeochemical cycling. The decline in sea-ice extent and thickness favors a longer open-water period with impacts on phytoplankton dynamics. Arctic net productivity is influenced by microalgae living associated with sea ice, with distinct species thought to be favored by ice-covered and ice-free waters. In this study, we investigated the phytoplankton community structure in Baffin Bay, a semi-enclosed sea where Arctic and North Atlantic water masses interact. We compared communities from the ice-free Atlantic-influenced eastern, the marginal ice zone, and the ice-covered Arctic-influenced western Baffin Bay. The community was characterized using 18S rRNA high-throughput amplicon sequencing and flow cytometry cell counting, and compared to environmental data collected during the Green Edge campaign. We sampled 16 stations grouped by sectors according to sea-ice cover. In the sectors associated with sea ice, phytoplankton formed a highly diverse community of smaller taxa, which contrasted with a low-diversity community in ice-free sectors, dominated by larger centric diatoms and *Phaeocystis pouchetii* adapted to high light/low nutrient conditions. Several phytoplankton species were flagged as indicators for the under-ice and marginal ice zone sectors, including ice-associated taxa such as the diatoms *Melosira arctica* and *Pseudo-nitzschia seriata*, but also subspecies representatives of the early-blooming alga *Micromonas polaris* and the cryptophyte *Baffinella frigidus*. The strong association of certain taxa with under-ice and marginal ice zone sectors, including *Pterosperma* sp., *Chrysochromulina* sp., *Micromonas polaris*, and *B. frigidus*, suggest that they might be indicators of diversity loss due to ongoing sea-ice changes in Baffin Bay. We report new intra-species variability of *Micromonas polaris* suggesting that seasonal specialists could wax and wane over the bloom and non-bloom periods, highlighting the need for detailed year-long studies and the importance of microdiversity when assessing the diversity and distribution of polar phytoplankton.

Keywords: Polar phytoplankton, Microbial eukaryotes, Arctic Ocean, Microdiversity, *Micromonas polaris*, *Baffinella frigidus*

1. Introduction

The recognition of the occurrence of under-ice phytoplankton communities in the Arctic Ocean (Arrigo et al., 2012; Arrigo et al., 2014) has represented a paradigm shift that has impacted the estimates of primary production (Kinney et al., 2020), as well as the understanding of biogeochemical cycling in the region (Ardyna et al., 2020). The Arctic is

undergoing drastic changes directly linked to sea-ice decline in both extent and thickness (Serreze et al., 2007; Meredith et al., 2019), fostering the early development of extensive under-ice phytoplankton (Horvat et al., 2017). A recent model indicates that the transmission of photosynthetically active radiation (PAR) through first- and second-year sea ice could sustain net phytoplankton growth over much of the Arctic by July (Ardyna et al., 2020). The periods when sea ice is present have been shortened by earlier melt and delayed freeze-up, lengthening the productive season (Tedesco et al., 2019) and impacting the timing of the characteristic phytoplankton spring blooms at the ice edge (Perrette et al., 2011; Janout et al., 2016; Renaut et al., 2018), with cascading effects to higher trophic levels and nutrient fluxes (Leu et al., 2011; Post et al., 2013).

Phototrophic communities in high-latitude environments are subjected to a light regime dictated by seasonally restricted solar energy input and factors that

¹GEMA Center for Genomics, Ecology & Environment, Universidad Mayor, Camino La Pir amida, Huechuraba, Santiago, Chile

²Department of Biosciences, University of Oslo, Oslo, Norway

³Sorbonne Universit , CNRS, UMR7144, Team ECOMAP, Station Biologique de Roscoff, Roscoff, France

⁴D partement de Biologie, Institut de Biologie Int grative et des Syst mes, Universit  Laval, Quebec, QC, Canada

* Corresponding author:

Email: catherine.gerikas@gmail.com

attenuate light, including sea-ice extent and thickness, and snow cover (Leu et al., 2015). The sea ice also provides a complex habitat for the sympagic community (Niemi et al., 2011), with a “seeding” role from older to first-year sea-ice (Olsen et al., 2017; Kauko et al., 2018) and to the water column during ice melt (Hardge et al., 2017). The sympagic community has been associated with higher abundance and better nutrition for pelagic zooplankton and higher trophic levels (Hop et al., 2011; Schmidt et al., 2018). Arctic sea ice harbors complex communities with diverse metabolic strategies, where different types of ice promote different community structures (Comeau et al., 2013). Sea ice may act as a flagellate cyst repository, for example, for dinoflagellates such as *Polarella glacialis* (Kauko et al., 2018). Sympagic assemblages, which may harbor still unknown but potentially important protist taxa (Hardge et al., 2017; Ribeiro et al., 2020), are now threatened due to the rapid decline in ice extent. A drastic decrease in sympagic protist diversity has been reported in the Arctic due to the loss of multiyear sea ice, which has almost 40% more diatom species than first-year ice (Hop et al., 2020).

Apart from sea-ice loss, the “Atlantification” phenomenon represents another risk to the Arctic ecosystem. First reported more than a decade ago (Hegseth and Sundfjord, 2008), the Atlantification of Arctic waters has hydrographic impacts on the stratification of the water column and sea-ice decline due to increased heat fluxes from Atlantic Water (Polyakov et al., 2017), as well as biological impacts via advection of temperate species (Neukermans et al., 2018; Oziel et al., 2020). Several studies also report a phytoplankton downsizing trend in warmer ocean waters (Morán et al., 2010; Hilligsoe et al., 2011). For example, warm anomalies in the Atlantic Water inflow to the Arctic Ocean appear to shift plankton dominance from diatom cells to small coccolithophores (Smyth et al., 2004; Lalande et al., 2013). Studies have reported that increasing Arctic temperatures and water column stratification, as well as ocean acidification, will also favor specific pelagic populations, such as the pico-sized green alga *Micromonas polaris* (Li et al., 2009; Hoppe et al., 2018; Benner et al., 2019).

Diatoms tend to dominate sympagic communities and are reported in under-ice blooms in the Arctic, especially pennate diatoms of the genera *Nitzschia*, *Fragilariopsis*, *Navicula*, and *Cylindrotheca* (Leu et al., 2015; Ardyna et al., 2020; Hop et al., 2020), with *Nitzschia frigida* reported as the main taxon within bottom-ice communities (Croteau et al., 2022) and during the polar winter (Niemi et al., 2011). As the snow melts during spring and summer, the formation of melt ponds creates a new habitat that can be connected to the water column below. Melt pond communities are often dominated by flagellates (Mundy et al., 2011) and mixo/heterotrophic groups, including Chrysophyceae, Filosa-Thecofilosea, and ciliates (Xu et al., 2020). The bottom-ice communities are the most biologically rich, characterized by the presence of pennate diatoms and the strand-forming centric diatom *Melosira arctica* (Poulin et al., 2014). The seasonally retreating marginal ice zone is followed by massive

phytoplankton blooms developing close to and below the ice edge (Perrette et al., 2011). Open water phytoplankton are composed of different diatom communities compared to that of sea ice (Oziel et al., 2019), with a greater presence of centric diatoms such as *Thalassiosira* and *Chaetoceros*, which are more adapted to the lower concentrations of nutrients and the higher light levels within the ice-free euphotic zone (Morando and Capone, 2018; Kvernvik et al., 2020).

In addition to diatoms, other groups also play a pivotal role in the Arctic ecosystem. The Arctic picophytoplankton (0.2–2 μm) is dominated by the Mamiellophyceae *Micromonas polaris*, *Bathycoccus prasinus*, and *Mantoniella* spp. (Not et al., 2005; Lovejoy et al., 2007; Joli et al., 2017). *Micromonas polaris* is often the most abundant (Lovejoy and Potvin, 2011; Balzano et al., 2012) and is considered an Arctic sentinel species (Freyria et al., 2021) due to the close relationship of its distribution patterns with temperature (Demory et al., 2019). Besides the pan-Arctic importance of Mamiellophyceae, Baffin Bay seems to hold a high degree of endemism within this class (Ibarbalz et al., 2023). *Phaeocystis* is a globally distributed haptophyte genus, with a high impact on carbon and sulfur exchange at the ocean/atmosphere interface (Schoemann et al., 2005). The bloom-forming species *P. pouchetii* has a pan-Arctic distribution (Lasternas and Agust, 2010), with blooms detected even under thick snow-covered pack ice (Assmy et al., 2017). The cryptophyte *Baffinella frigidus* (Daugbjerg et al., 2018) was described from a strain isolated from northern Baffin Bay in 1998 (CCMP2045) and isolated again, from both water and ice samples, in the same region (Ribeiro et al., 2020). Cryptophytes are important members of polar phytoplankton communities (Terrado et al., 2013; Hamilton et al., 2021), and their association with sea ice in the Arctic (Comeau et al., 2013; Piososz et al., 2013) might represent a vulnerability as ongoing Arctic warming trends intensify.

Baffin Bay is a seasonally ice-covered sea within the Canadian Arctic, with a complex interplay of water masses of Arctic, Atlantic, and Pacific origin. The longitudinal physicochemical gradient created by this system results in distinct stratification patterns (Randelhoff et al., 2019) and differential sea-ice melt rates (Tang et al., 2004), greatly impacting the structure of the food web and carbon export (Saint-Béat et al., 2020), as well as the permeability of the sea ice, influencing brine connectivity and nutrient availability to sympagic algae (Tedesco et al., 2019). Baffin Bay is especially susceptible to drastic environmental changes, with a reported increase in the length of the melt season by 20 days compared to 4 decades ago (Stroeve et al., 2014). The increase is associated with ongoing warming on Baffin Bay eastern subsurface boundaries caused by Atlantic inflow and freshening trends in Arctic-influenced sectors (Zweng and Münchow, 2006).

In the present work, we used high-throughput amplicon sequencing and a microdiversity approach (one base-pair resolution in sequence analysis) to investigate how the phytoplankton community structure changes across the marginal ice zone between the Atlantic-influenced eastern and the Arctic-influenced western Baffin Bay. This

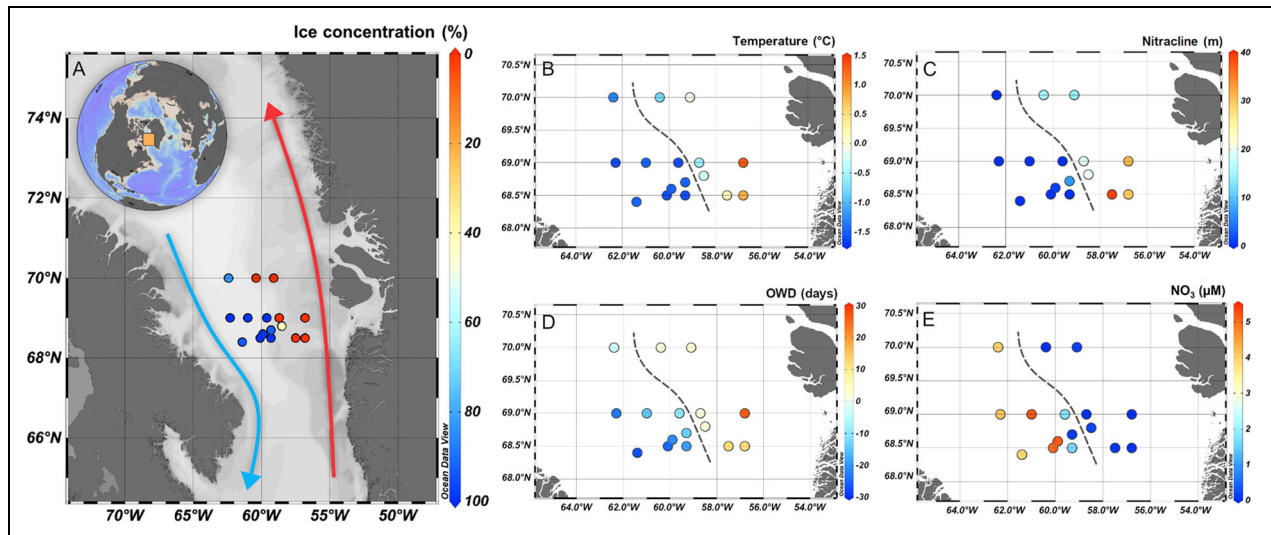


Figure 1. Location of the sampling stations in Baffin Bay and environmental variables. (A) Sampling stations indicating sea-ice concentration (%) and the warmer West Greenland Current (red arrow) and cooler Pacific-originated Baffin Current (blue arrow); (B) temperature ($^{\circ}\text{C}$) in surface water; (C) depth (m) of the nitracline; (D) Open Water Days (OWD), that is, number of days of open water before (positive values) or after (negative values) the sampling day; and (E) nitrate concentration (μM) in surface water. A dashed line separates sampling stations with more than (western) and less than (eastern) 80% sea-ice cover.

study provides high-resolution profiling of the phytoplankton community between under-ice and open-water environments and highlights the vulnerability of these communities to sea-ice decline down to the subspecies level. For the purpose of the present work, we consider the term “subspecies” to comprise intraspecific genetic variability, meaning small changes in the 18S rRNA V4 region that were detected over time and space within a given species. Populations bearing persistent minor genetic differences might indicate the existence of ecotypes adapted to different niches, adding complexity and resilience to a given ecosystem (Needham and Fuhrman, 2016).

2. Materials and methods

2.1. Study area

Baffin Bay, a seasonally ice-covered sea within the Canadian Arctic, is delimited by Greenland in the east and Baffin Island in the west. The more temperate and salty West Greenland Current (WGC), a product of the interaction of North Atlantic waters with the Irminger Current, flows northward along the Greenland coast and eastern Baffin Bay, entering the Davis Strait in mid-Baffin Bay (Tang et al., 2004). Due to its higher density, and the dominating flow from the Canadian Archipelago from west to east, the WGC cannot pass through the archipelago and recirculates counterclockwise, interacting with the colder, less saline, Pacific-originated Arctic waters, flowing southward as the Baffin Island Current (BIC; Jones et al., 2003; Münchow et al., 2015, **Figure 1**). Sea-ice formation starts in Baffin Bay during October and covers almost all of its area by March, followed by the onset of the melting season in April, as the sea ice retreats westward until it reaches a minimum extent by August/

September (Tang et al., 2004). In western Baffin Bay, the onset of snow-cover melt modulates the end of the sea-ice algal bloom and the beginning of the under-ice phytoplankton spring bloom (Oziel et al., 2019).

2.2. Sampling and DNA extraction

Seawater samples were collected in four longitudinal transects across the marginal ice zone, from open waters (eastern Baffin Bay) to several kilometers into the pack ice (western Baffin Bay), onboard the research icebreaker CCGS *Amundsen*. Sampling was carried out between 68.4°N – 70°N and 56.8°W – 62.4°W , from June 9 to July 2, 2016, for a total of 16 sampling stations (**Figure 1**). At each station, seawater was sampled at 6 depths within the euphotic layer, ranging from 0 m (surface water) to 75 m (Data S1), using 12-L Niskin bottles mounted on a rosette system equipped with a Seabird SBE-911plus CTD unit (Sea-Bird Electronics, Bellevue, WA, USA). The list of the sensors attached to the rosette carousel can be found in Bruyant et al. (2022). From each sampling depth, 3 L of water were pre-filtered with a $100\ \mu\text{m}$ mesh and subsequently filtered with a peristaltic pump through the following sets of polycarbonate filters: $20\ \mu\text{m}$ (47 mm), $3\ \mu\text{m}$ (47 mm), and $0.22\ \mu\text{m}$ (SterivexTM filters) to study the structure of the phytoplankton community in each size fraction. Although pre-filtration of seawater samples might exclude diatoms and colonies larger than $100\ \mu\text{m}$, it prevents the over-representation of metazoan reads in the dataset. Filters were placed in cryotubes (except for the SterivexTM), preserved with 1.8 mL of RNAlaterTM, and stored at -80°C until processing. DNA was extracted using ZR Fungal/Bacterial DNA MiniPrep (Zymo Research, Irvine, CA, USA) following manufacturer’s instructions, and final concentrations were measured

using PicoGreen™ (Thermo Fisher Scientific, Waltham, MA, USA) with a LabChip GX (Perkin-Elmer, Waltham, MA, USA).

2.3. 18S rRNA V4 PCR amplification and sequencing

The V4 hypervariable region of the 18S rRNA gene (about 380 bp) was amplified using the V4 primers TAR-euk454FWD1 (forward, 5'-CCAGCASCYGGTAATCC-3'; Stoeck et al., 2010) and V4 18S Next.Rev (reverse, 5'-ACTTTCGTTCTTGATYRATGA-3'; Piredda et al., 2017), together with the Illumina Nextera 5' end overhang sequence (Illumina, San Diego, CA, USA) as described in Piredda et al. (2017). Reaction mixtures in a total of 20 μ L were performed using 10 μ L of Phusion High-Fidelity PCR Master Mix® 2 \times , 0.3 μ M final concentration of each primer, 3% DMSO, 2% BSA, and H₂O. Thermal conditions were as follows: 98°C for 5 min, followed by 25 cycles of 98°C for 20 s, 52°C for 30 s, 72°C for 90 s, and a final cycle of 72°C for 5 min. Samples were amplified in triplicate and pooled together subsequently to minimize the chance of amplification errors. PCR purification was performed using AMPure XP Beads (Beckman Coulter, Brea, CA, USA) following instructions from the manufacturer. DNA quantification and the quality check was done using a LabChip GX Touch HT Nucleic Acid Analyzer (PerkinElmer, Waltham, MA, USA). Libraries were prepared as detailed on the Illumina® support website (<http://support.illumina.com>) with a final concentration of 1 nM and 1% denatured PhiX to prevent sequencing errors due to low-diversity libraries. Sequencing was performed using a 2 \times 50 bp MiSeq Reagent Kit v2® at the GenoMer platform (Roscoff, France).

2.4. Sequence processing

Sequences were processed using the *dada2* (Callahan et al., 2016) package within R (R Core Team, 2021). Reads were filtered and trimmed using the *filterAndTrim* function with the following parameters: *truncLen* = c(250, 240), *trimLeft* equal to each primer length (for primer removal), *maxN*=0, *maxEE*=c(2, 2), and *truncQ*=10. Merging of forward and reverse reads with the *mergePairs* function and chimeric sequences removal with the *removeBimeraDenovo* function were both performed with default parameters. Resulting ASVs were taxonomically assigned using *assignTaxonomy* function with the PR² database (Guillou et al., 2013) version 4.12 (<https://pr2-database.org/>). Samples with less than a total of 3,000 reads were excluded, and the number of reads for each sample was normalized by the median sequencing depth. Autotrophic taxa were selected by filtering-in divisions Chlorophyta, Cryptophyta, Haptophyta, and Ochrophyta. Within these divisions, genera known to comprise only heterotrophic members (e.g., *Spumella*) were excluded. Dinoflagellates were not considered in the present study as they comprise both autotrophic and heterotrophic taxa and have a high number of 18S rRNA gene copies, which tend to dominate read numbers, obscuring patterns of other autotrophs. The processing script can be found at https://github.com/vaulot/Paper-2021-Vaulot-metapr2/tree/main/R_processing.

2.5. Environmental data

Environmental variables were collected during the Green Edge campaign (Lafond et al., 2019; Randelhoff et al., 2019; Saint-Béat et al., 2020, Table S1). All ancillary physico-chemical and biological data obtained from the Green Edge project are available as raw data (Massicotte et al., 2019) and as formatted files (Massicotte et al., 2020). The data are described in detail by Bruyant et al. (2022); those used in the analyses of this study are provided in Data S1 (see Data Availability section). The complete list of variables sampled during the Amundsen Green Edge campaign, the principal investigator responsible for each dataset, and the protocols used to obtain and analyze physical, chemical, and biological data can be found in Bruyant et al. (2022). Further information on pigments, nutrients, particulate organic carbon, and particulate organic nitrogen concentrations can be found in Lafond et al. (2019), Burgers et al. (2020), and Joy-Warren et al. (2023). Ammonium determination was performed in the field using 20 mL of seawater, following Holmes et al. (1999). Urea concentration was determined at room temperature following Goeyens et al. (1998). Data processing for light transmittance, sea-ice cover, and water column stability can be found in Randelhoff et al. (2019). The Arctic Nitrate-Phosphate tracer (ANP) was used for water mass characterization, as calculated by Randelhoff et al. (2019) following Newton et al. (2013). In short, differences in the N/P ratio are used to define the origin of a given water mass, using linear regressions specific to the Arctic water column. ANP values close to zero or close to one are indicative of signatures of Atlantic-originated and Pacific-derived water masses, respectively.

2.6. Flow cytometry analysis

The abundance of autotrophic (chlorophyll-containing) cells was measured *in situ* using a BD Accuri™ C6 flow cytometer as previously described (Marie et al., 2010; Ribeiro et al., 2016). Pico-phytoplankton (0.2 μ m to 2 μ m) and nano-phytoplankton (2 μ m to 20 μ m) abundance was measured on unstained samples with fluorescent beads for parameter normalization (0.95 μ m G Fluoresbrite® Polysciences, Warrington, PA), while heterotrophic cell enumeration was performed using SYBR Green® staining as described in Marie et al. (1997). Cryptophyte abundance was estimated using its distinct phycoerythrin orange fluorescence. Other phycoerythrin-containing taxa, such as *Synechococcus*, can be identified by distinctive cytogram distribution patterns and were not present in our analysis. Rhodophytes are filtered out by pre-filtration with a 100 μ m mesh at the moment of sampling.

2.7. Data analysis

Sampling stations (Figure 1) were clustered into open water (OW), marginal ice zone (MIZ), and under-ice (UI) stations using sea-ice cover dynamics based on the parameter open water days (OWD). OWD correspond to how many days a given station had been ice-free before sampling (positive values) or how many days passed before it became ice-free after sampling (negative values; see Randelhoff et al., 2019). Stations with OWD >10 were

Table 1. Stations with their geographical coordinates, Julian day, ice-related characteristics, and size fractions analyzed

Station	Longitude	Latitude	Day	Sector ^a	Ice Cover (%)	OWD ^b	Size Fractions (μm)
G100	-56.8	68.5	161	OW	0	12	0.2–3, >20
G102	-57.5	68.5	162	OW	0	12	0.2–3, >20
G107	-59.3	68.5	163	UI	100	-19	0.2–3, >20
G110	-60.1	68.5	164	UI	100	-25	0.2–3, 3–20, >20
G115	-61.4	68.4	165	UI	93	-27	0.2–3, 3–20, >20
G201	-59.9	68.6	166	UI	99	-21	0.2–3, 3–20, >20
G204	-59.3	68.7	167	UI	93	-14	0.2–3, 3–20, >20
G207	-58.5	68.8	168	MIZ	41	2	0.2–3, 3–20, >20
G300	-56.8	69	169	OW	0	26	0.2–3, 3–20, >20
G309	-58.7	69	170	MIZ	0	2	0.2–3, 3–20, >20
G312	-59.6	69	171	MIZ	100	-10	0.2–3, 3–20, >20
G318	-61	69	172	UI	99	-15	0.2–3, 3–20, >20
G324	-62.3	69	173	UI	100	-23	0.2–3, 3–20, >20
G507	-59.1	70	182	MIZ	0	3	3–20, >20
G512	-60.4	70	183	MIZ	0	2	3–20, >20
G519	-62.4	70	184	MIZ	84	-3	3–20, >20

^aOpen water (OW), under ice (UI), and marginal ice zone (MIZ).

^bOpen water days (OWD): number of days ice-free before sampling (positive) or to become ice-free after sampling (negative).

considered OW, stations with OWD 10 to -10 were considered within the MIZ, and stations with OWD < -10 were considered UI (Table 1). The number of samples collected within each sector and size fractions analyzed can be found in Table 2.

Data analysis was performed within R, using the following packages: *phyloseq* (data filtering, heatmaps, alpha diversity; McMurdie and Holmes, 2013), *tidyr* (data wrangling; Wickham et al., 2019), *vegan* (nonmetric multidimensional scaling, NMDS; Dixon, 2003), and *ggplot2* (plotting; Wickham, 2016). Abundant amplicon sequence variants (ASVs) for each size fraction were selected by keeping only ASVs that were among the top 90% most abundant reads in at least one sample. Abundant taxa for the whole community (i.e., considering all size fractions) had to be among the top 90% most abundant sequences in at least 10% of the samples. Abundance filtering was performed with the *topf* and *genefilter_sample* functions in *phyloseq*. NMDS analysis was performed using Bray-Curtis distance with the *metaMDS* function of the package *vegan*, and statistically significant environmental parameters (p -value ≤ 0.001) and genera (p -value ≤ 0.05) were mapped against it using the function *envfit*. Indicator species analysis (*indicspecies* package; De Cáceres et al., 2010) was performed with abundant taxa (selected as described above) within each size fraction to find a significant association between taxa and a given sector (or combination of sectors), using the default *IndVal* index as statistic test and 9,999 random permutations. Global distribution of

Table 2. Number of samples within each of the sectors, Under Ice (UI), Marginal Ice Zone (MIZ), and Open Water (OW), for each size fraction

Sector	0.2–3 μm	3–20 μm	20 μm
UI	40	35	40
MIZ	18	28	34
OW	16	5	18

Micromonas polaris ASV_0003 and ASV_0154, and *Baffinella frigidus* ASV_0041, ASV_0055, and ASV_0346 was carried out using metaPR² web-based tool (<https://shiny.metapr2.org>; Vaultot et al., 2022). The metaPR² database contains metabarcodes from 59 public datasets representing more than 6,000 samples distributed over a wide range of ecosystems. ASV sequences from the present study were entered in the “Query” panel, and matching metaPR² ASVs (100% similarity) were displayed in the “Map” panel.

3. Results

Here we present the results of sampling seawater across the marginal ice zone in Baffin Bay, Arctic, June 9 to July 2, 2016, to assess changes in the phytoplankton community, taxonomically from division to subspecies level, as related to sea-ice cover and the physico-chemical gradients between the Atlantic-influenced

eastern and Arctic-influenced western Baffin Bay. Analyses of the plankton community are based on three, sequentially filtered size fractions (0.2–3 μm , 3–20 μm , and >20 μm) and their sampling stations, classified according to sea-ice cover as UI, MIZ, and OW (Tables 1 and 2).

3.1. Physical, chemical, and biological variability

The seawater temperature was lower in the Arctic-influenced UI sector and higher in terms of both absolute values and median in the Atlantic-influenced OW sector. Temperature differences between the two sectors were statistically significant (levels of significance can be found in Figures 1 and 2A). Salinity did not differ significantly between the two ice-influenced UI and MIZ sectors, with a wider distribution toward less saline sampling depths influenced by sea-ice melt. Salinity values were less variable in the OW sector, ranging narrowly between 33.6 and 34.0 (Figure 2B, Data S1). Chlorophyll fluorescence was higher in the MIZ and the well-irradiated OW sectors, reaching a peak in the former sector with 14.5 mg m^{-3} (Figure 2C). The mixed layer depth (MLD) differed significantly between the UI and OW sectors, being deeper in the UI sector, where it varied from 27 m to 46 m. UI and OW were also distinct from MIZ, with the MLD ranging from 4 m to 12 m (Figure 2D). PAR ($\text{mol photons}^{-2} \text{d}^{-1}$) was not significantly different between MIZ and OW, although variability was greater in the MIZ, in accordance with the variable ice cover (Figure 2E).

The nitracline depth differed significantly between sectors, generally deeper in the OW sector, and always below 30 m. In the UI sector, it was never deeper than 8 m, while in the MIZ sector the nitracline depth was variable, with values ranging from 0 m to 20 m (Figure 2F). Nutrient concentrations in general were higher in the UI sector compared to the MIZ and OW sectors. The MIZ was more similar to OW than UI for all nutrients (Figure S1A–F) and nutrient ratios measured (Figure S1G–I). Nitrate, phosphate, silicic acid, colored dissolved organic matter, and urea concentrations differed significantly between the UI and OW sectors, with maximum values higher in the UI sector compared to the OW and MIZ sectors (levels of significance can be found in Figures S1 and S2). Particulate organic nitrogen and carbon also differed significantly between the UI and OW sectors, but maximum values were considerably higher in the MIZ sector (Figure S2). Particulate organic nitrogen concentrations may represent overestimations due to the presence of inorganic nitrogen on the filters, which was considered to be negligible. Urea concentrations were higher in the UI sector, reaching 1.9 μM , almost double the maximum concentration found in other sectors (Figure S2A). Although ammonium concentrations were significantly different between UI and OW, maximum concentrations of up to 0.8 μM were found in the MIZ sector (Figure S2B). Ammonium assimilation and regeneration differed significantly between the three sectors, with higher median values found in the MIZ sector (Figure S2G–H). In contrast, urea assimilation decreased in the UI sector and nitrate assimilation was somewhat even among all sectors (Figure S2I–J). Dissolved organic nitrogen and primary production were higher in the MIZ

sector, although the highest values for the latter were in the UI sector, up to 88 $\mu\text{g C L}^{-1} \text{day}^{-1}$ (Figure S2L). The ANP relationship was higher close to the western boundary of Baffin Bay, indicating the presence of Arctic, Pacific-originated waters in this region (Figure S3).

3.2. Phytoplankton abundance

Phytoplankton abundance measured by flow cytometry revealed different distributional patterns between pico (0.2–3 μm) and nano (3–20 μm) size fractions (Figure 2G–H). Pico-phytoplankton abundance was greatest in the UI sector (up to $39 \times 10^3 \text{ cells mL}^{-1}$) and lowest in the OW sector ($0.95 \times 10^3 \text{ cells mL}^{-1}$ on average; Figure 2G). Differences between sectors were highly significant for the smallest size fraction, unlike nano-phytoplankton, where only UI and OW extremes differed significantly. The abundance of nano-phytoplankton was highest in the MIZ sector (up to $22 \times 10^3 \text{ cells mL}^{-1}$), although the median was the highest in OW (Figure 2H). The abundance of cryptophytes differed significantly between all sectors, with much higher values in the UI sector (up to 182 cells mL^{-1}) than in the MIZ and especially the OW sector, where they were virtually absent (Figure 2I). Pico- and nano-phytoplankton abundance was generally highest in surface waters in the UI sector, while appearing relatively constant over the sampling depths in OW (Figure 3). Within the MIZ, pico-phytoplankton abundance was higher in surface and subsurface waters, while nano-phytoplankton peaked in deeper samples. Cryptophyceae abundance in the UI sector was generally higher in surface/subsurface waters, although some elevated abundances also appeared in deeper samples (Figure 3).

3.3. Phytoplankton diversity at the division and genus level

Community composition at the division level had a marked difference between sectors, especially for the smaller (0.2–3 and 3–20 μm) size fractions. The 0.2–3 μm size fraction was dominated mainly by Chlorophyta in the ice-associated sectors (UI and MIZ) throughout the sampled water column, with an important share of Cryptophyta and Ochrophyta, while in the OW sector, Haptophyta was predominant (Figure S4). In the 3–20 μm size fraction, Haptophyta relative abundance was higher in surface and sub-surface samples of the MIZ sector, and in deeper samples of the OW sector (Figure S4). Ochrophyta dominated the >20 μm size fraction in all three sectors, with only a small increase in the relative abundance of Haptophyta for the MIZ and OW sectors (Figure S4).

At the genus level, community composition in the 0.2–3 μm size fraction did not differ greatly in any sector from that observed at the division level, because the two most abundant divisions, Chlorophyta and Haptophyta, were dominated by the genera *Micromonas* and *Phaeocystis*, respectively (Figure 4). Within Mamielophyceae, *Bathycoccus* and *Mantoniella* were detected mainly in ice-associated sectors, the former with higher relative abundances in the deeper samples and the

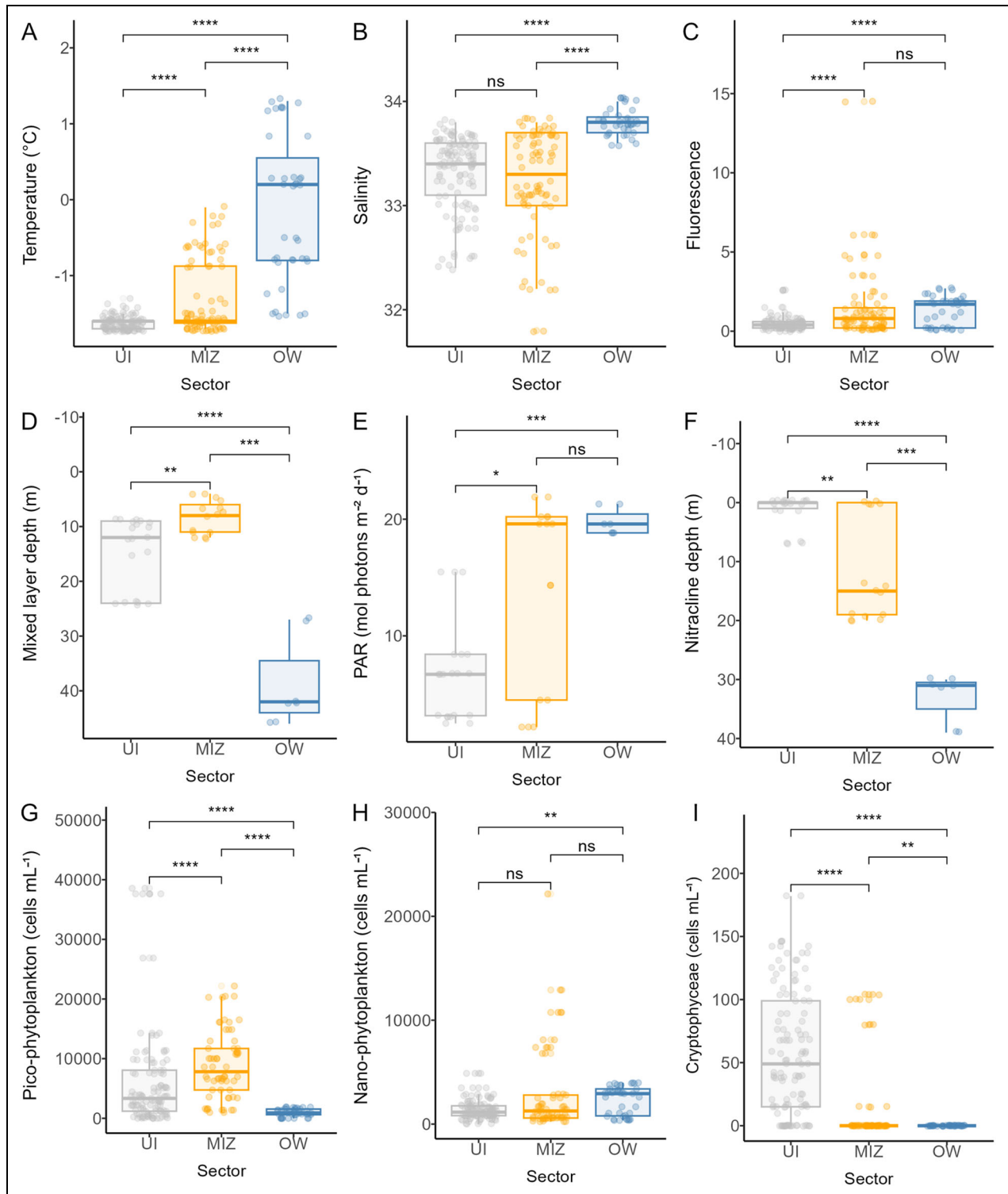


Figure 2. Environmental variables for the three sampling sectors. Environmental variables for the Under Ice (UI, gray), Marginal Ice Zone (MIZ, yellow), and Open Water (OW, blue) sectors: (A) temperature (°C); (B) salinity; (C) chlorophyll fluorescence; (D) mixed layer depth (m); (E) photosynthetically active radiation (PAR) at 3 m (mol photons m⁻² d⁻¹); (F) nitracline depth (m); (G) pico-phytoplankton abundance (cells mL⁻¹); (H) nano-phytoplankton abundance (cells mL⁻¹); and (I) Cryptophyceae abundance (cells mL⁻¹). The plots for each sector indicate the data (color-coded points) and the median (horizontal line), range (vertical line), quartiles (box limits), and outliers. Individual observation points are shown with horizontal spread (jittering) to avoid overlap. Panels A–C and G–I include data from all depths sampled, surface to 75 m. The *p*-values, obtained with the Wilcox test, are indicated as follows: *p* ≤ 0.05 (*); *p* ≤ 0.01 (**); *p* ≤ 0.001 (***); *p* ≤ 0.0001 (****); and not significant (ns).

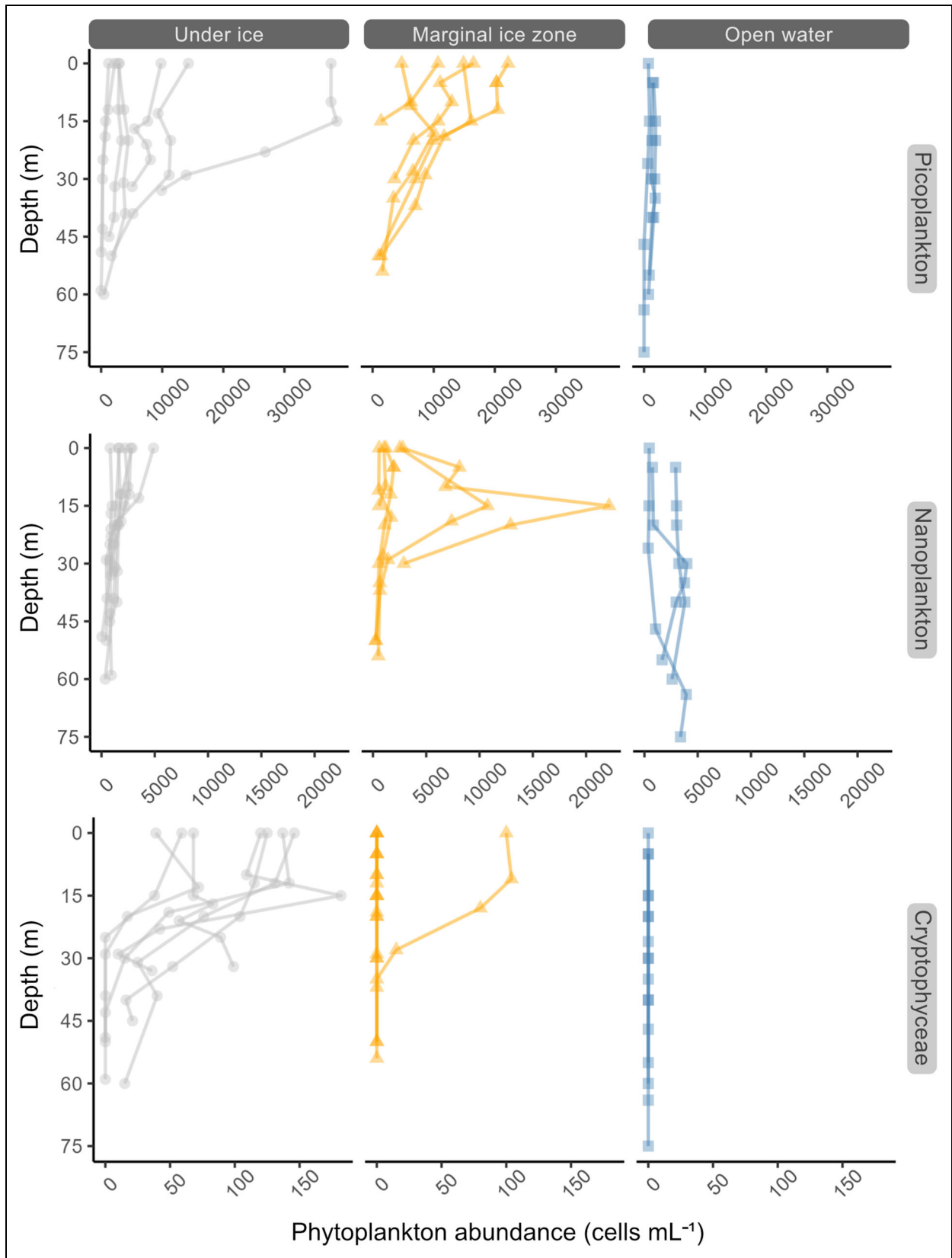


Figure 3. Abundance of pico-phytoplankton, nano-phytoplankton, and Cryptophyceae cells in the three sampling sectors. Abundance (cells mL⁻¹), measured by flow cytometry, of pico-phytoplankton (top panels), nano-phytoplankton (middle panels), and Cryptophyceae (lower panels) according to depth, divided between the three sectors: under ice (gray), marginal ice zone (yellow), and open water (blue).

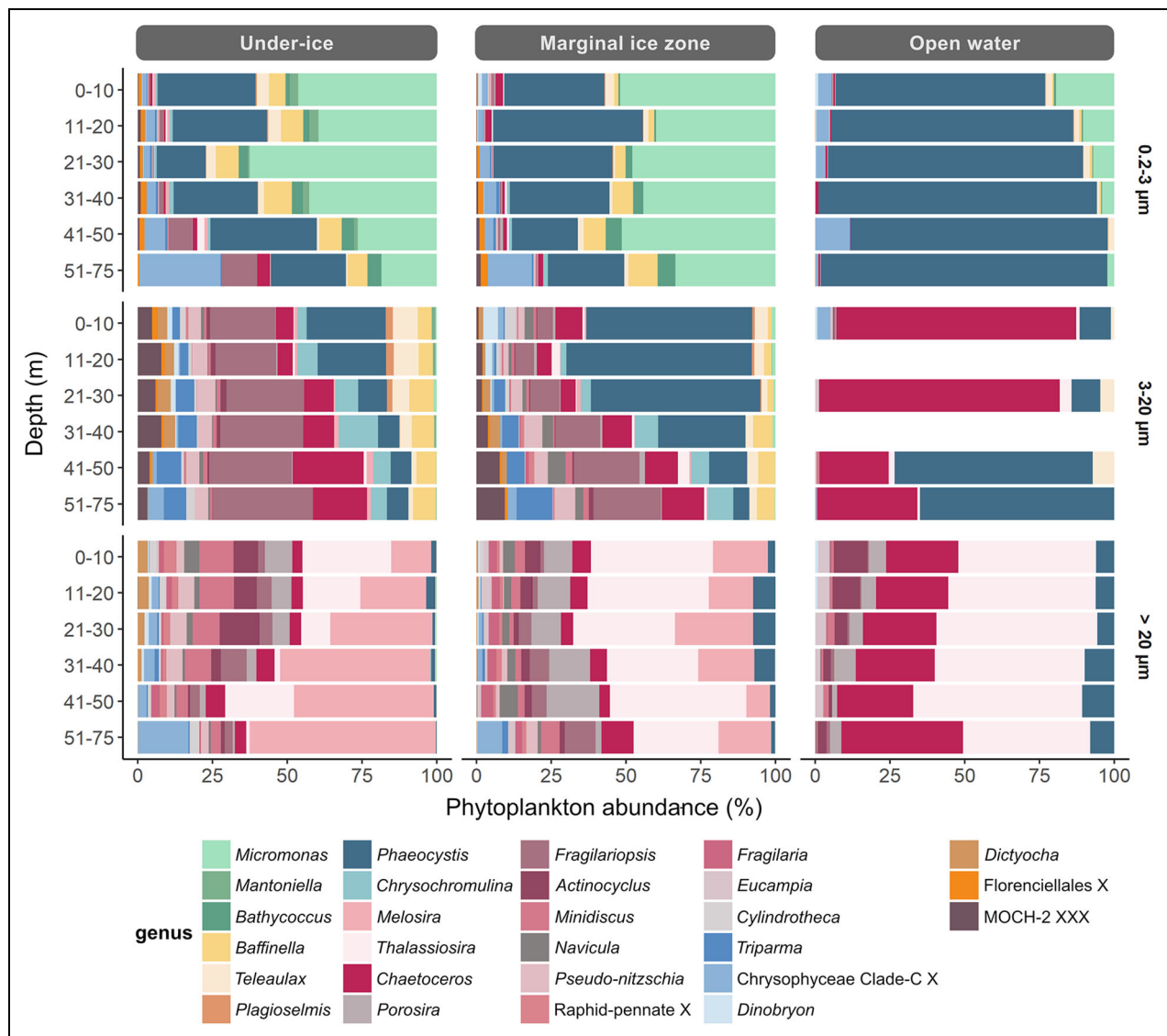


Figure 4. Relative abundance of phytoplankton at the genus level. Relative abundance of reads at the genus level between size fractions across the three sampling sectors: under-ice, marginal ice zone, and open water. Genera are grouped by classes (e.g., Mamiellophyceae, Cryptophyceae, etc.). There are no samples for the depths 11–20 m and 31–40 m in the 3–20 µm size fraction of the open water sector. Note that the deeper interval covers a greater range of depths (from 51 m to 75 m) due to fewer samples in this lower limit.

latter in surface samples. Cryptophyta were dominated mainly by *Baffinella* in UI and MIZ and by *Teleaulax* in the OW sector. Although not abundant, Bacillariophyceae (diatoms) were extremely diverse in the ice-associated sectors (Figure 4). The decrease in *Baffinella* in the OW sector is corroborated by the large drop in Cryptophyceae abundance within this sector as measured by flow cytometry (Figure 2G).

Mamiellophyceae were nearly absent in the 3–20 µm size fraction, except for a small contribution to surface samples in the UI and MIZ sectors. A higher contribution of *Chrysochromulina* within Haptophyta was observed in the ice-associated sectors, especially in deeper samples (Figure 4). Among cryptophytes, a higher abundance of *Teleaulax* relative to *Baffinella* was observed in the 3–20 µm in comparison to the 0.2–3 µm size fraction, especially in surface samples. As observed in the smallest size fraction, Ochrophyta

were fairly diverse in the ice-associated sectors, with representatives of Bacillariophyceae, Bolidophyceae, Dictyochophyceae, and Marine Ochrophyta (MOCH-2). The diatom *Chaetoceros* was dominant in the OW sector, especially in surface samples, with a small contribution of *Thalassiosira*.

There was a decrease in non-diatom Ochrophyta representatives in the >20 µm size fraction, although *Dictyocha* and *Triparma* were still present in the ice-associated sectors, the former mostly in surface and the latter in deeper samples (Figure 4). Regarding diatoms, there was an increase in *Porosira*, *Actinocyclus*, and especially *Thalassiosira* in all the sectors in comparison with other size fractions, and in *Melosira* relative abundance in ice-associated sectors.

NMDS analysis revealed that samples clustered according to size fractions along the first axis and sectors along the second axis. The UI and MIZ sectors were associated

with the presence of Pacific-originated Arctic waters, a higher concentration of nutrients, and higher cell abundance of Cryptophyceae, while the OW sector presented higher temperatures and the use of alternative nitrogen sources, such as urea and ammonium (**Figure 5A**). Statistically significant genera had a distribution related to both sectors and size fractions. For example, pennate diatoms such as *Pseudo-nitzschia* and *Cylindrotheca* were correlated with larger size fractions from ice-associated samples, while *Baffinella*, *Bathycoccus*, and *Micromonas* were correlated with smaller fractions of the same samples. Centric diatoms such as *Thalassiosira*, *Chaetoceros*, and *Eucampia* were associated with larger size fractions from the OW sector, and *Phaeocystis* with smaller size fractions.

3.4. Phytoplankton microdiversity

Taxa grouped by genera masked the variability at the species and ASV levels. Looking at all genera with more than two ASVs in the whole dataset, the ASV-level distribution of taxa suggests some niche preference. Most genera had more ice-associated ASVs than OW (**Table 3**). Interestingly, several low-abundance taxa included many ice-associated ASVs, for example, the Dictyochophyceae genus *Pseudochattonella* and environmental clade 2 of Bolidophyceae. Two groups had a surprisingly large number of ASVs: clade B of Dolichomastigaceae (Mamiellophyceae) with a total of 28 ASVs, and the centric diatom genus *Chaetoceros* with 35 ASVs (**Table 3**). Alpha diversity indices indicate that, in general, diversity was higher in the smallest size fraction in the UI and MIZ sectors and decreased toward larger size fractions. However, the Simpson index was lowest in the 3–20 μm size fraction and the highest in the >20 μm size fraction (Figure S5).

In order to find patterns of taxa distribution that could be used as ecological indicators of niche preferences, we analyzed ASV distribution in each sector and group of sectors using indicator species analysis (De Cáceres et al., 2010). This approach identified 72 ASVs that were representative (highly significant association, $p < 0.001$) of one or two sectors across all size fractions (**Tables 4** and S2). Within the 0.2–3 μm size fraction, 20 representative ASVs were related to the UI (7; **Table 4**) or the MIZ+UI sectors (13; Table S2). In the 0.2–3 μm size fraction, among the highly significant taxa within the UI sector were four Ochrophyta (three diatoms and one Pelagophyceae). Thirteen ASVs were highly correlated to the MIZ+UI sector, including two Mamiellophyceae (*Bathycoccus prasinos* and *Micromonas commoda* A2), two cryptophytes, both assigned to *Baffinella frigidus*, seven non-diatom Ochrophyta, and two diatoms (*Pseudo-nitzschia seriata* and *Chaetoceros neogracilis*). A *Micromonas polaris* ASV (ASV_0154) was also considered an indicator of the MIZ+UI sector, with a p -value of 0.0013 (Table S2).

The six ASVs that were considered indicators of the UI sector in the 3–20 μm size fraction had lower p -values, with *Pterosperma* sp. (p -value = 0.0099) reaching the highest association score (Table S2). Considering only highly significant associations (p -value < 0.001), *Navicula* sp. (ASV_0049) was the only ASV representative of the MIZ, while several Ochrophyta and one Cryptophyta

member were identified as indicators from the MIZ+UI sector, all of them also highly significant related to ice-associated sectors in the 0.2–3 μm size fraction (**Table 4**). Two centric diatoms were significantly associated with the OW sector, *Thalassiosira* sp. (ASV_0057) and *Chaetoceros rostratus* (ASV_0177; **Table 4**).

Of the 31 highly significant indicator ASVs found in the >20 μm size fraction, only one was related to the UI (*Pseudo-nitzschia seriata*, ASV_0046), one to the MIZ (*Entomoneis ornata*, ASV_0259), and three to the OW sector (*Chaetoceros contortus* ASV_0334, *Chaetoceros diadema* 1 ASV_0407, and Chrysophyceae Clade-H ASV_0156; **Table 4**). Fifteen ASVs were highly related to the MIZ+UI sector (Table S2), including the two *Melosira arctica* ASVs (0009 and 0025). Of the 11 indicator ASVs strongly associated with the MIZ+OW sector (Table S2), 10 were centric diatoms, including four *Chaetoceros*, four *Thalassiosira*, one *Eucampia* sp., and one *Detonula confervacea* (ASV_0137). Interestingly, the most abundant ASV in the whole dataset, *Phaeocystis pouchetii* (ASV_0001), was also highly related to the MIZ+OW sector in the >20 μm size fraction (Table S2).

3.5. Distribution of abundant ASVs

Although few genera and undescribed groups dominated the community, the distribution of the 10 most abundant ASVs in each division across the sectors followed distinct patterns within these genera and even within the same species (**Figure 6**). For example, within the top 10 most abundant Cryptophyta ASVs, three were assigned to *Baffinella frigidus*. While *B. frigidus* ASV_0041 was strongly associated with MIZ+UI samples for both 0.2–3 and 3–20 μm size fractions but also found in the OW sector, ASV_0055 was found exclusively in ice-associated sectors in the smaller size fraction (**Figure 6**). A third *B. frigidus* (ASV_0346) was found only at stations with >90% sea-ice cover (**Figure 6**). Interestingly, although the three *B. frigidus* ASVs have few differences in the V4 region of the 18S rRNA gene (Figure S6), their distribution in the metaPR², a database of eukaryotic 18S rRNA ASVs with an emphasis on protists, follows a similar pattern, with ASV_0041 as the most abundant with widespread distribution, ASV_0346 as the least abundant with a restricted distribution constrained to higher latitudes, and ASV_0055 some intermediate both in terms of abundance and distribution range (Figure S7). In contrast, some ASVs probably represent generalist species as they were present (and abundant) throughout the dataset, regardless of environmental differences between sectors, such as *Micromonas polaris* (ASV_0003), *Teleaulax glacialis* (ASV_0038), and *Phaeocystis pouchetii* (ASV_0001; **Figure 6**).

The top 10 Chlorophyta ASVs belonged to five genera: *Bathycoccus*, *Mantoniella*, *Micromonas*, *Pterosperma*, and *Pyramimonas*, of which five ASVs were significantly correlated with ice-associated sectors. *M. polaris* ASV_0154 had a single base pair difference with *M. polaris* ASV_0003 (Figure S8) and was less abundant than the latter in our dataset (**Figure 6**), as well as in other Arctic datasets (Figure S9). *M. squamata* (ASV_0104) and *Pterosperma* sp.

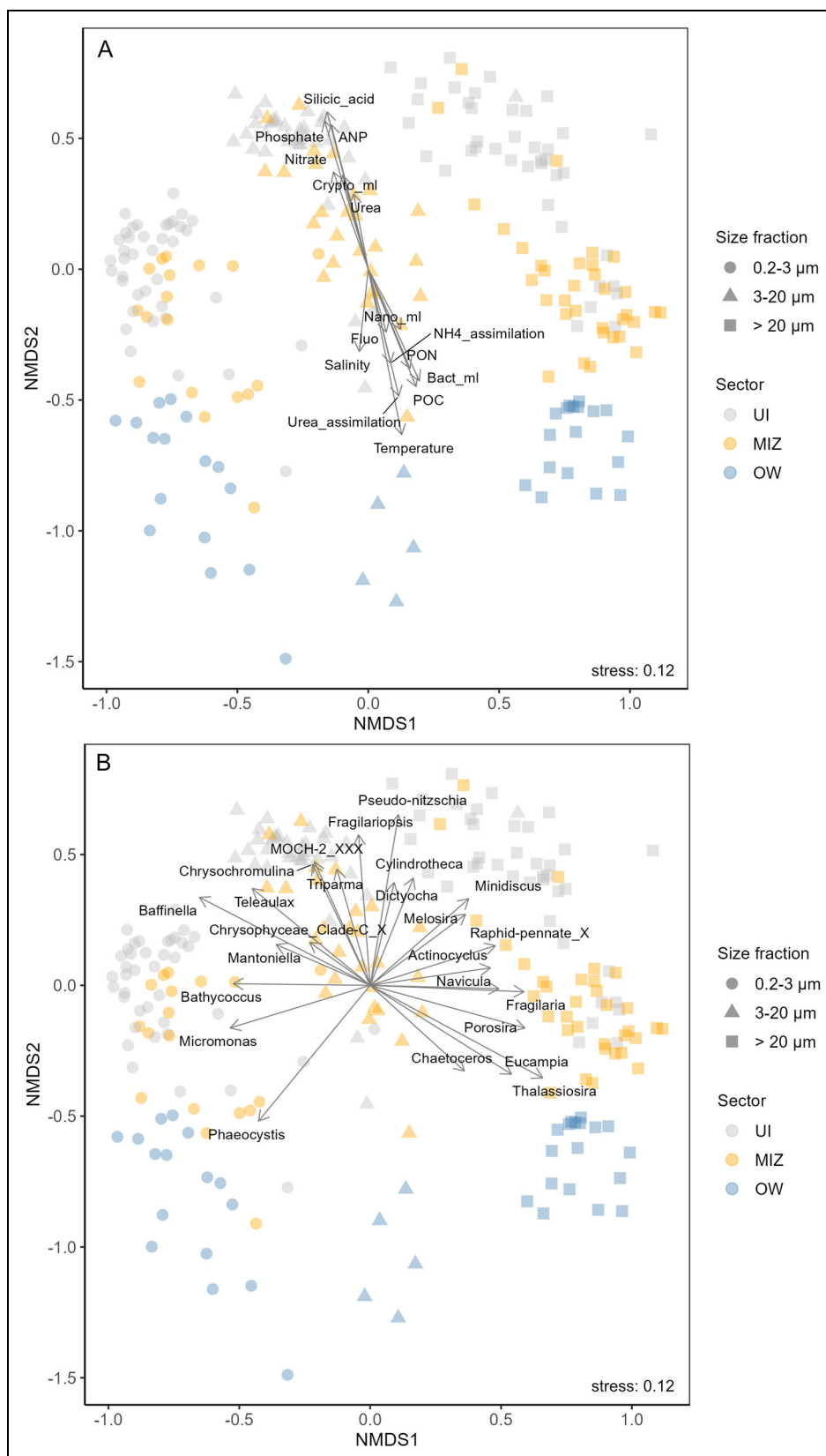


Figure 5. Nonmetric multidimensional scaling (NMDS) analysis based on phytoplankton size fraction and sampling sector. NMDS analysis using Bray–Curtis dissimilarities of the phytoplankton community composition, where only statistically significant (A) environmental parameters (p -value = 0.001) and (B) genera (p -value = 0.05) were plotted against ordination. Parameters in panel A are bacterial abundance (Bact_ml), Cryptophyceae abundance (Crypto_ml), chlorophyll fluorescence (Fluo), nano-phytoplankton abundance (Nano_ml), concentrations of nitrate, silicic acid, particulate organic carbon (POC), particulate organic nitrogen (PON), and phosphate, Arctic N-P relationship (ANP), ammonium assimilation rate (NH4_assimilation), urea concentration (Urea) and assimilation rate (Urea_assimilation), salinity, and temperature. Stress: 0.12.

Table 3. Number of amplicon sequence variants by phytoplankton genera and undescribed clades present in the Under-Ice (UI), Marginal Ice Zone (MIZ) and Open Water (OW) sectors, considering only taxa with more than 2 ASVs in the whole dataset

Division	Class	Genus ^a	UI	MIZ	OW	Total
Chlorophyta	Mamiellophyceae	Dolichomastigaceae-B	14	11	11	28
Chlorophyta	Mamiellophyceae	<i>Micromonas</i>	5	6	3	7
Chlorophyta	Pyramimonadales	Pyramimonadales XXX	4	4	2	4
Chlorophyta	Pyramimonadophyceae	<i>Pterosperma</i>	3	1	1	4
Chlorophyta	Pyramimonadophyceae	<i>Pyramimonas</i>	7	6	3	8
Cryptophyta	Cryptophyceae	<i>Baffinella</i>	5	3	1	5
Cryptophyta	Cryptophyceae	Goniomonadales XX	3	0	1	4
Cryptophyta	Cryptophyceae	<i>Plagioselmis</i>	1	3	1	3
Cryptophyta	Cryptophyceae	<i>Rhodomonas</i>	3	3	2	4
Cryptophyta	Cryptophyceae	<i>Teleaulax</i>	3	1	1	3
Haptophyta	Haptophyta Clade HAP4	Haptophyta Clade HAP4 XXX	3	0	0	3
Haptophyta	Haptophyta X	Haptophyta XXXX	3	2	0	3
Ochrophyta	Bacillariophyta	<i>Actinocyclus</i>	6	6	2	9
Ochrophyta	Bacillariophyta	<i>Bacillaria</i>	6	5	2	7
Ochrophyta	Bacillariophyta	<i>Chaetoceros</i>	19	26	22	35
Ochrophyta	Bacillariophyta	<i>Cylindrotheca</i>	2	3	1	5
Ochrophyta	Bacillariophyta	<i>Ditylum</i>	3	1	0	3
Ochrophyta	Bacillariophyta	<i>Entomoneis</i>	6	2	1	6
Ochrophyta	Bacillariophyta	<i>Fragilaria</i>	3	3	1	3
Ochrophyta	Bacillariophyta	<i>Fragilariopsis</i>	3	3	2	3
Ochrophyta	Bacillariophyta	<i>Melosira</i>	3	4	1	5
Ochrophyta	Bacillariophyta	<i>Minidiscus</i>	3	3	2	3
Ochrophyta	Bacillariophyta	<i>Navicula</i>	3	2	2	3
Ochrophyta	Bacillariophyta	Naviculales	5	2	1	5
Ochrophyta	Bacillariophyta	<i>Pleurosigma</i>	3	1	0	3
Ochrophyta	Bacillariophyta	<i>Pseudogomphonema</i>	3	1	0	3
Ochrophyta	Bacillariophyta	<i>Pseudo-nitzschia</i>	2	4	3	4
Ochrophyta	Bacillariophyta	Raphid-pennate X	7	8	1	8
Ochrophyta	Bacillariophyta	<i>Stauroneis</i>	2	3	0	3
Ochrophyta	Bolidophyceae	Parmales env 1 X	4	3	1	5
Ochrophyta	Bolidophyceae	Parmales env 2 X	5	1	0	6
Ochrophyta	Bolidophyceae	Parmales env 3 X	2	1	0	3
Ochrophyta	Bolidophyceae	<i>Triparma</i>	3	3	2	6
Ochrophyta	Chrysophyceae	Chrysophyceae Clade-C X	6	6	2	8
Ochrophyta	Chrysophyceae	Chrysophyceae Clade-D X	0	3	0	3
Ochrophyta	Chrysophyceae	Chrysophyceae Clade-F X	4	2	2	6
Ochrophyta	Chrysophyceae	Chrysophyceae Clade-H X	23	6	6	24
Ochrophyta	Chrysophyceae	Chrysophyceae Clade-I X	3	0	2	4
Ochrophyta	Chrysophyceae	Chrysophyceae XXX	3	1	1	3

(continued)

Table 3. (continued)

Division	Class	Genus ^a	UI	MIZ	OW	Total
Ochrophyta	Chrysophyceae	<i>Paraphysomonas</i>	3	2	1	3
Ochrophyta	Dictyochophyceae	<i>Pseudochattonella</i>	6	4	1	6
Ochrophyta	MOCH-1	MOCH-1 XXX	3	1	0	3
Ochrophyta	MOCH-2	MOCH-2 XXX	5	4	0	6

^aTaxa not assigned to the genus level (e.g., those containing Xs such as Pyramimonadales XXX) might contain more than one genus.

Table 4. Amplicon Sequence Variants (ASVs) that were highly significant indicators ($p < 0.001$) for a single sector, with their taxonomic assignment, according to size fraction (see full data in Table S2)

Size Fraction (μm)	Sectors ^a	ASVs	Class	Species	A ^b	B ^c	Stat ^d	p-value
0.2–3	UI	asv_00015	Bacillariophyta	<i>Fragilariopsis cylindrus</i>	0.93	0.75	0.83	0.0001
0.2–3	UI	asv_00009	Bacillariophyta	<i>Melosira arctica</i>	0.98	0.70	0.83	0.0003
0.2–3	UI	asv_00171	Bacillariophyta	Raphid–pennate X sp.	0.97	0.68	0.81	0.0001
0.2–3	UI	asv_00104	Mamiellophyceae	<i>Mantoniella squamata</i>	1.00	0.48	0.69	0.0002
0.2–3	UI	asv_00311	Pelagophyceae	<i>Ankylochrysis</i> sp.	0.96	0.48	0.67	0.0007
0.2–3	UI	asv_00125	Prymnesiophyceae	<i>Phaeocystis</i> sp.	0.93	0.75	0.84	0.0001
0.2–3	UI	asv_00244	Pyramimonadophyceae	<i>Pterosperma</i> sp.	1.00	0.43	0.65	0.0002
>20	UI	asv_00046	Bacillariophyta	<i>Pseudo-nitzschia seriata</i>	0.79	0.85	0.82	0.0001
3–20	MIZ	asv_00049	Bacillariophyta	<i>Navicula</i> sp.	0.82	0.89	0.85	0.0007
>20	MIZ	asv_00259	Bacillariophyta	<i>Entomoneis ornata</i>	0.83	0.62	0.72	0.0001
0.2–3	OW	asv_00156	Chrysophyceae	Chrysophyceae Clade–H X sp.	0.81	0.88	0.84	0.0001
0.2–3	OW	asv_00248	Chrysophyceae	Chrysophyceae Clade–H X sp.	0.86	0.94	0.90	0.0001
0.2–3	OW	asv_00666	Chrysophyceae	Chrysophyceae Clade–I X sp.	1.00	0.38	0.61	0.0002
0.2–3	OW	asv_00593	Dictyochophyceae	Pedinellales X sp.	1.00	0.50	0.71	0.0001
0.2–3	OW	asv_00731	Dictyochophyceae	Pedinellales X sp.	1.00	0.31	0.56	0.0002
0.2–3	OW	asv_00421	Mamiellophyceae	Dolichomastigaceae–B sp.	0.89	0.44	0.62	0.0002
3–20	OW	asv_00177	Bacillariophyta	<i>Chaetoceros rostratus</i>	0.83	1.00	0.91	0.0002
3–20	OW	asv_00057	Bacillariophyta	<i>Thalassiosira</i> sp.	0.92	0.80	0.86	0.0002
>20	OW	asv_00334	Bacillariophyta	<i>Chaetoceros contortus</i>	0.72	0.83	0.77	0.0001
>20	OW	asv_00407	Bacillariophyta	<i>Chaetoceros diadema 1</i>	0.82	0.67	0.74	0.0001
>20	OW	asv_00156	Chrysophyceae	Chrysophyceae Clade–H X sp.	0.99	0.28	0.53	0.0006

^aUnder ice (UI), marginal ice zone (MIZ), and open water (OW).

^bThe positive predictive power of the ASV; that is, the probability of a sampling site being a member of the sector or group of sectors when the ASV appears in that site.

^cHow often one ASV is found in sampling sites of the sector or group of sectors.

^dValue of the correlation.

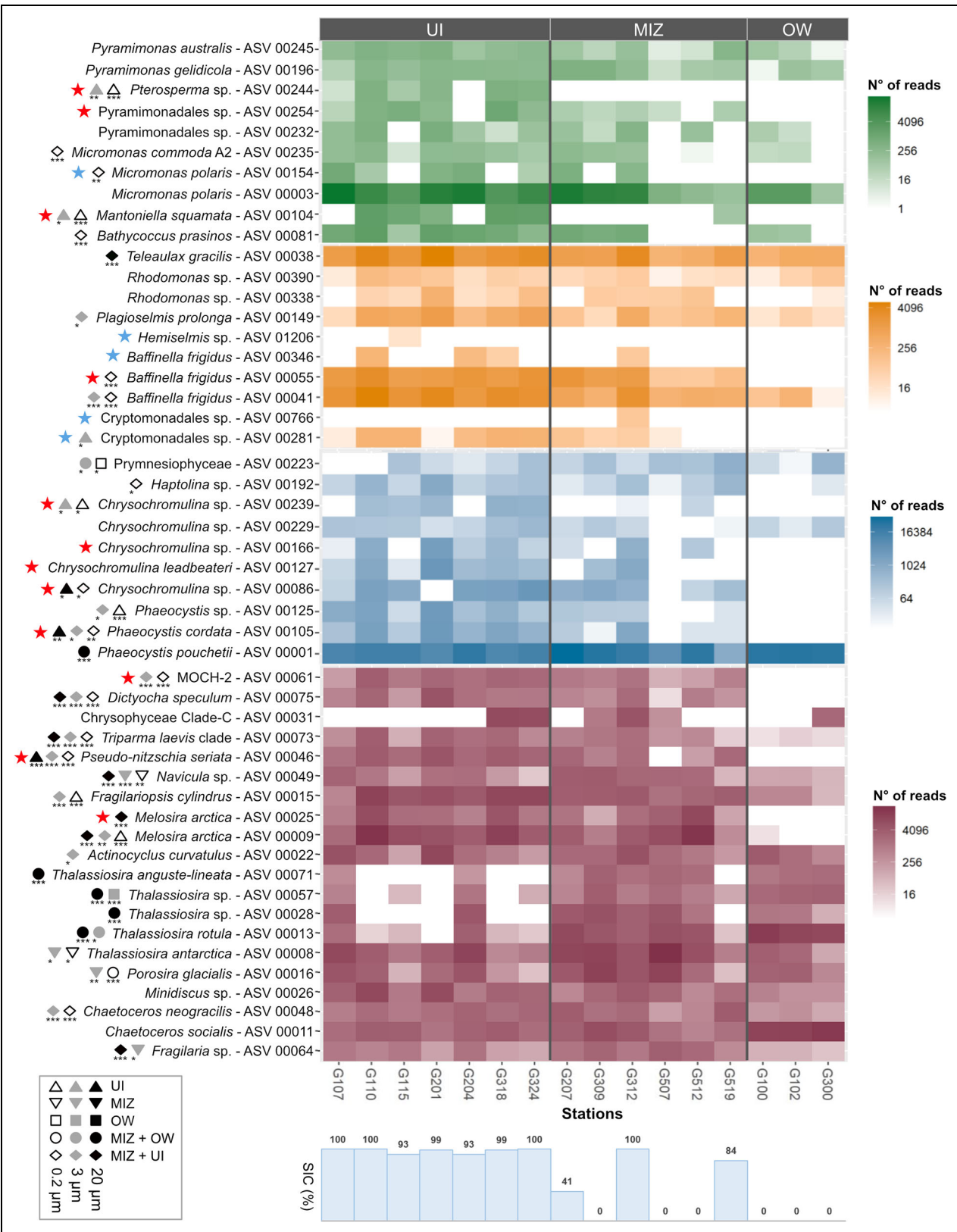


Figure 6. Main distribution of phytoplankton taxa by sampling sector. Distribution of the most abundant taxa (amplicon sequence variants, ASVs) for each station within each sampling sector, under ice (UI), marginal ice zone (MIZ), and open water (OW). The top 10 ASVs were selected within the Chlorophyta (green), Cryptophyta (orange), and Haptophyta (blue), and the top 20 most abundant within the highly diverse Ochrophyta division (red). Symbols indicate if a given ASV was reported as indicator ASV for the UI (triangles), MIZ (inverted triangles), OW (squares), MIZ+UI (diamonds), or MIZ+OW (circles) sector groups within 0.2–3 μm (white), 3–20 μm (grey) or >20 μm (black) size fractions. Asterisks indicate the *p*-values associated with the indicator ASV: 0 (***) , 0.001 (**), and 0.01 (*). Red and blue stars indicate if a given ASV was found exclusively in ice-associated sectors, with blue stars meaning the ASVs were not abundant. Sea-ice concentration (SIC) is also indicated for each sampling station.

(ASV_0244) were present only in the UI sector, mainly within the 0.2–3, but also in the 3–20 μm size fraction.

Five *Chrysochromulina* and three *Phaeocystis* ASVs comprised the 10 most abundant Haptophyta, three of them found only in the ice-associated sectors. Interestingly, *P. cordata* ASV_0105 and *Phaeocystis* sp. ASV_0125 were strongly associated with both UI and MIZ+UI sectors, while *P. pouchetii* ASV_0001 was associated with the larger size fraction of MIZ+OW, although highly abundant at all stations (Figure 6).

The most abundant non-diatom Ochrophyta were MOCH-2 ASV_0061, *Dictyocha speculum* ASV_0075 and *Triparma laevis* ASV_0073, all of them flagged as ice-associated indicator ASVs in all size fractions, except for MOCH-2 which was not an indicator for the >20 μm size fraction (Figure 6). Many diatoms were flagged as indicator species for ice-associated sectors, including pennate diatoms such as *Pseudo-nitzschia seriata*, *Navicula* sp., and *Fragilaria* sp., and centric diatoms such as *Melosira arctica* and *Chaetoceros neogracilis*. Interestingly, of the five *Thalassiosira* ASVs ranked as the most abundant Ochrophyta, four were considered indicator species of the OW or MIZ+OW sectors, while *Thalassiosira antarctica* was mainly associated with the smaller size fractions of the MIZ sector, although present in all sectors. *Teleaulax gracilis* ASV_0038 was highly abundant in all sectors but was flagged as an indicator ASV for the MIZ+UI sector in the >20 μm size fraction. Other abundant centric diatoms were also indicators of the MIZ+OW sectors, such as *Eucampia* sp. ASV_0079 and *Polarella glacialis* ASV_0016 ASV_0073 (Figure 6).

4. Discussion

4.1. General eastern and western Baffin Bay structure

The Green Edge campaign consisted of east-west transects that captured the transition zone between eastern Baffin Bay, influenced by the Atlantic-origin WGC water mass, and the colder, less saline BIC in the Arctic-influenced western Baffin Bay (Lafond et al., 2019; Randelhoff et al., 2019; Saint-Béat et al., 2020; Vilgrain et al., 2021). Such transition was corroborated by ANP tracer calculation in the stations from the present study (Figure S3), and is even more evident in the extended ANP dataset provided by Randelhoff et al. (2019). The transects also captured the dynamics of sea-ice retreat, which in Baffin Bay develops from east to west, mostly due to the presence of the warmer waters of Atlantic origin in its eastern sector (Tang et al., 2004). In general, our data corroborated previous studies regarding environmental conditions and the main phytoplankton groups in the region (Lafond et al., 2019; Oziel et al., 2019). In the sea-ice-covered UI sector, characterized by lower light (Figure 2) and higher nutrient concentrations (Figure S1), we observed a community diversity skewed toward sympagic diatoms and non-diatom Ochrophyta (Figure 5). As previously reported for ice-free Arctic regions, the OW sector was characterized by a deeper nitracline (Figure 2), the use of alternative sources of nitrogen (Figure 5A), and a community dominated by larger centric diatoms adapted to a high light/

low nutrient environment (Figure 5B). Jacquemot et al. (2022) observed that the transition from under-ice communities dominated by pico-sized phytoplankton to open-water stations characterized by larger phytoplankton thriving at the subsurface chlorophyll maxima has cascading effects on the microbial food webs, impacting carbon and energy export. Saint-Béat et al. (2020) reported that the interplay of different water masses producing the east-west gradients in Baffin Bay led to contrasting environments with distinct biogeochemical functionings, with the west characterized by higher carbon export.

In ice-covered areas subjected to pre-bloom conditions, photosynthetic activity is limited by light availability, with shade-acclimated under-ice populations (Ardyna et al., 2020). During the Green Edge campaign, light availability and vertical mixing allowed the initiation of the bloom under nearly 100% sea-ice cover (UI sector). Still, the bloom peaked in terms of chlorophyll *a* approximately 10 days after ice retreat (Randelhoff et al., 2019), near the limit between the MIZ and OW sectors. In the present study, the relatively stable community composition between the UI and MIZ sectors, which corresponded roughly to the peak of the bloom identified by Randelhoff et al. (2019), may be explained by the seeding of taxa through ice-melt waters (Mundy et al., 2011) combined with the “priming” effect suggested by Lewis et al. (2019). The “priming” effect arises from the acclimation of pre-bloom, under-ice communities to low and highly variable light input due to patchy snow cover and melt pond/open water lead formation, resulting in a competitive advantage to rapidly exploit increasing irradiation (Lewis et al., 2019). The MIZ sector showed evidence of increased biological activity: pico- and nanophytoplankton abundance, dissolved and particulate organic carbon concentration, particulate organic nitrogen concentration, dissolved organic nitrogen, and primary production, in general, were higher in the MIZ than in the UI or OW sectors (Figures 3, S1, and S2). Also, Vilgrain et al. (2021) reported that near the ice edge, copepods were heavily pigmented due partially to full gut contents, in a region with high chlorophyll *a* concentrations (Lafond et al., 2019).

As ice cover decreases and sea-ice melts, the community must transition from light-limited conditions, characteristic of a pre-bloom state, to a high-light, nutrient-limited environment (Lewis et al., 2019). The nitracline deepened from the surface in the UI sector to more than 30 m in OW, along with the development of a subsurface chlorophyll *a* maximum (Randelhoff et al., 2019), as a result of the rapid consumption of inorganic nutrients in surface waters, following an expected trend in Arctic plankton dynamics (Martin et al., 2010; Ardyna et al., 2020). In classic post-bloom conditions, new production is confined to deeper layers, and the euphotic layer is then dominated by regenerative production (Sakshaug, 2004) and the use of alternative nitrogen sources, such as found in the OW sector (Figure 5A). Within ice-free Arctic waters, species may also be subjected to the detrimental effects of high UV exposure resulting in low cell viability and a decline in photosynthetic performance, a scenario allowing, in

general, centric diatoms to out-compete other microalgae (Alou-Font et al., 2016; Kvernvik et al., 2020). Lafond et al. (2019) reported that the subsurface chlorophyll *a* maximum in the eastern, Atlantic-influenced Baffin Bay was dominated by *Chaetoceros* and *Thalassiosira*, as also found in the present study (**Figure 5B**). These results might explain the relative decline in non-diatom Ochrophyta in OW. The increase in *Chaetoceros* spp. in the OW sector, especially within the 3–20 μm size fraction in the upper waters, may reflect an ecological advantage within a post-bloom scenario, as this genus has a high growth rate irrespective of nitrogen source in polar (Schiffrine et al., 2020) and subtropical (Morando and Capone, 2018) environments. Croteau et al. (2022) observed that photoadaptation is key to understanding the Arctic seasonal succession of diatoms, as late-bloom species such as *C. neogracilis* are prone to higher productivity and lower vulnerability to photoinhibition in comparison to sentinel sympagic diatoms like *Nitzschia frigida*.

4.2. Indicator species and microdiversity

Using a microdiversity approach in this study, we report how distinct environmental variables found in Baffin Bay impact phytoplankton community composition down to the subspecies level. Different ASVs within the same species can represent distinct ecotypes, leading to resilience and adaptation of microbial populations under changing environmental conditions (Needham and Fuhrman, 2016; García-García et al., 2019) and the persistence of particular lineages over time. For example, Sjöqvist and Kremp (2016) reported that genetic diversity within diatom species ensured an optimized ecological performance, including carbon uptake and overall resistance to environmental changes.

Ice-associated stations, most still covered with sea ice and categorized as low-productivity stations by Lafond et al. (2019), harbored the most diverse community, from the genus to the ASV level, within each size fraction (**Figure 4** and **Table 3**). Overall, our flow cytometry and metabarcoding data point to a great importance of smaller size fractions within ice-associated sectors in terms of cell abundance and overall plankton diversity. Under-ice communities are adapted to low-light environments, capable of maximizing light absorption by increasing intracellular concentrations of accessory and photosynthetic pigments (Matsuoka et al., 2009; Lewis et al., 2019). Recruitment under dark polar conditions might explain the dominance of *Micromonas* within the UI and MIZ sectors, as they are early bloom taxa (Lovejoy et al., 2007) with known persistence during winter (Vader et al., 2015; Joli et al., 2017).

The most striking difference between ASV distribution patterns among dominant species in the present study was observed within *Micromonas polaris* and *Baffinella frigidus* populations (**Figure 6**). The Chlorophyta genus *Micromonas* is diverse and widely distributed from coastal to oceanic waters through all the global latitudinal ranges (Simon et al., 2017; Tragin and Vaultot, 2019). The genus *Micromonas* exhibits a wide thermal niche and is considered a sentinel for polar (Freyria et al., 2021) and global plankton diversity (Demory et al., 2019) in relation to

temperature changes in the oceans. The *M. polaris* CCMP2099 strain isolated from the North Water Polynya (Lovejoy et al., 2007) and the RCC2306 strain from the Beaufort Sea (holotype of the species; Simon et al., 2017) are 100% similar in the V4 region of the 18S rRNA gene to the *M. polaris* ASV_0003 from the present study. *M. polaris* ASV_0003 has a widespread distribution pattern with a high abundance in all sectors (**Figure 6**), following its dominant role within the Arctic (Lovejoy et al., 2002; Not et al., 2005; Lovejoy et al., 2007; Balzano et al., 2012). Although *M. polaris* ASV_0154 differs from ASV_0003 by a single nucleotide (Figure S8), its distinct distribution (**Figure 6**) and the assignment of ASV_0154 (and not ASV_0003) as an ice-associated indicator species suggest that it might represent a previously unresolved ecotype.

The use of metabarcoding datasets combined with microdiversity approaches has previously enabled the discovery of new polar *Micromonas* ecotypes, such as the *Micromonas* B3 clade, which shows a wider distribution toward lower latitudes than *Micromonas polaris* (Tragin and Vaultot, 2019). *M. polaris* ASV_0154 does not have any 100% similarity match in GenBank, either to strains or environmental sequences. The distribution of *M. polaris* ASV_0154 is pan-Arctic, although it always contributes to a small fraction of *Micromonas* reads (Figure S9). *M. polaris* ASV_0154 has also been found in the Nares Strait (metaPR² set #42; Figure S9; Kalenitchenko et al., 2019), which is connected to northern Baffin Bay and is responsible for southward transport of waters and ice from the Arctic Ocean into the region (Tang et al., 2004). Using a decade-long 18S rRNA data series focused on later summer to late autumn samples, Freyria et al. (2021) identified *M. polaris* as a summer specialist favored by nutrient-poor waters, in contrast to the present study, which identified the species either as a generalist, present in all sectors (ASV_0003), or as an ice-associated indicator ASV (ASV_0154). Our work highlights new intra-species variability of *M. polaris* suggesting seasonal specialists could wax and wane over the bloom and non-bloom periods and a need for detailed yearlong studies of polar phytoplankton ASVs.

Other Chlorophyta showed distinct occurrence patterns. *Pterosperma* sp. ASV_0244 was found exclusively in the UI sector and flagged as one of its few abundant indicator species (**Figure 6**). Although the genus *Pterosperma* has been reported from several regions within the Arctic (Lovejoy et al., 2002; Joli et al., 2017), with a preference for multiyear ice over first-year ice (Hop et al., 2020), ASV_0244 did not present a 100% match to any strain or environmental sequence in GenBank. *Pterosperma* sp. ASV_0244 was only found in seven high-latitude samples in the metaPR² database (data not shown).

As observed for *Micromonas polaris*, known cultured representatives of *Baffinella frigidus* such as CCMP2045 correspond to the most abundant and widespread ASV from *B. frigidus* of this study (ASV_0041; Figure S6). Strains 100% similar to the abundant and widespread *M. polaris* ASV_0003 and *B. frigidus* ASV_0041 were also isolated by Ribeiro et al. (2020) from Baffin Bay. Ibarbalz et al. (2023) reported that endemic Arctic taxa usually occur in relatively lower abundances. Although it could

be the result of randomness, the recurrent isolation of dominant subspecies highlights the need for new approaches for the isolation of microalgae to fully represent Arctic polar diversity in culture collections. New approaches would be particularly important for vulnerable taxa such as polar Cryptophyceae, which in general seem to have a tight relationship with sea ice (Comeau et al., 2013; Piwosz et al., 2013), decreasing rapidly in numbers when it melts (**Figure 3**).

The centric diatom *Melosira arctica* is an ice-associated taxon, forming long strands attached to the sea ice (Wassmann et al., 2006; Poulin et al., 2014) that are readily released as the ice melts, rapidly sinking and forming vast seafloor deposits (Boetius et al., 2013). Our data indicated two highly abundant *M. arctica* ASVs in the UI and MIZ sectors, the latter with several ice-free stations. Sampling roughly the same stations and using microscopy and pigment-based analysis, Lafond et al. (2019) showed that *M. arctica* in the MIZ was mainly in the form of actively silicifying resting spores, reaching up to 82% of biogenic silicic acid production. In the present study, abundant pennate diatoms, *Pseudo-nitzschia seriata* ASV_0046, *Navicula* sp. ASV_0049, and *Fragilaria* sp. ASV_0064, were all flagged as indicator species for ice-associated sectors. Interestingly, one of the most abundant *Chaetoceros* ASVs (*C. neogracilis* ASV_0048) was considered a highly significant ice-associated indicator ASV, but only for the smaller size fraction. *C. neogracilis* is a species complex with at least four known clades that share identical 18S rRNA sequences (Balzano et al., 2017), so the *C. neogracilis* distribution observed in the present study is likely masking finer clade-specific distributions. Furthermore, we recovered a total of 35 ASVs assigned to *Chaetoceros* (**Table 3**), indicating a high variability within this genus and a potentially higher resilience of this genus to a changing environment. Intra-species variability can influence the ecological success of diatoms, specially along environmental gradients (Sjöqvist and Kremp, 2016; Godhe and Rynearson, 2017).

Several abundant non-diatom ASVs were flagged as indicator ASVs for ice-associated sectors, especially in the smaller size fraction (**Figure 6**). Many of these indicator ASVs were found in datasets from the high Arctic, suggesting that UI and MIZ phytoplankton communities are highly diverse, probably low-light adapted populations of smaller organisms, which seem to be connected to higher latitude communities (Kalenitchenko et al., 2019) probably via water mass intrusions from the Nares Strait and the Smith, Jones, and Lancaster sounds (Tang et al., 2004; Bluhm et al., 2015). Among non-diatom Ochrophyta, we found high relative abundances of MOCH-2, *Dictyocha speculum*, the *Triparma laevis* clade, and an unidentified Florenciellales. The presence of the silicoflagellate *D. speculum* (synonym of *Octactis speculum*; Chang et al., 2017) in Arctic waters was first reported in the region more than a century ago (Lovejoy et al., 2002) and since regularly cited in the literature (Crawford et al., 2018). Its assignation as an indicator ASV for ice-associated sectors within all size classes in the present study might be a consequence of the presence of several life stages, including amoeboid, multinucleate, and

skeleton-bearing stages with different cell sizes (Moestrup and Thomsen, 1990; Chang et al., 2017).

The higher relative contribution of the haptophyte *Chrysochromulina* in deeper samples is consistent with previous reports linking this genus with deep chlorophyll maximum communities (Balzano et al., 2012). Many *Chrysochromulina* spp. ASVs were found exclusively or flagged as indicator taxa for ice-associated sectors. *Chrysochromulina* frequently occurs in sympagic communities and is considered one of the few ice-associated haptophytes (Mundy et al., 2011), but it is also present in ice-free waters from the Arctic (Lovejoy et al., 2002; Balzano et al., 2012) and the Antarctic (Luo et al., 2016; Trefault et al., 2021). The genus *Chrysochromulina* is morphometrically highly diverse (Egge et al., 2014) down to the subspecies level (Balzano et al., 2012; Needham and Fuhrman, 2016), and monitoring diversity should include high-resolution techniques to discern species/ecotypes distributions. Although not abundant in the present study, *Chrysochromulina* sp. ASV_0542 was found exclusively in under-ice samples. It was previously found to reach up to 2% of total eukaryotic reads in the Nares Strait (metaPR² set #42; Kalenitchenko et al., 2019) and was present in several stations from the Antarctic Peninsula (metaPR² set #387; Lin et al., 2021).

Phaeocystis pouchetii is ubiquitous throughout the Arctic (Schoemann et al., 2005; Lasternas and Agust, 2010) and has been reported to be capable of early blooms, even under snow-covered pack ice (Assmy et al., 2017). Although *P. pouchetii* ASV_0001 reads were present in all size fractions and sectors, the species was flagged as an indicator ASV for the MIZ+OW sector in the >20 μm size fraction. This finding could indicate the presence of *Phaeocystis* aggregates, which can be induced in the late stages of the spring bloom by senescent phytoplankton (Toullec et al., 2021), or the prevalence of large *P. pouchetii* colonies toward the eastern side of Baffin Bay. In general, blooming species of the genus *Phaeocystis* increase their C:N ratios under high-light, low-nutrient conditions, mainly through the production of a polysaccharide-based mucilaginous matrix, embedding colonies that reach up to 3 cm, which serve as energy storage and defense against grazers (Schoemann et al., 2005, and references therein). The dominance of the colonial form of *P. pouchetii* was reported during the Arctic 2007 ice-melt record (Lasternas and Agust, 2010), while the single-cell form was reported during overwintering (Vader et al., 2015). In a study covering Fram Strait and the Nansen Basin, Metfies et al. (2016) observed that the distributions of Phaeocystaceae and *Micromonas* were inversely correlated, the former more abundant in warmer Atlantic-influenced waters. The fact that *P. pouchetii* is adapted to grow in both nutrient-replete waters with 100% sea-ice cover, such as found in the UI sector, and the nutrient-depleted, high-light OW sector is consistent with earlier studies identifying this taxon as a potential winner for future Arctic scenarios, with implications for phytoplankton community structuring, trophic energy transfer, and carbon export (Wassmann et al., 2006; Verity et al., 2007; Lasternas and Agust, 2010).

5. Conclusions

In the present study, we report a difference in phytoplankton community structure related to different water masses and sea-ice cover in Baffin Bay. The sea-ice-covered western region, influenced by the southward flow of Pacific-origin Arctic waters, was characterized by a diverse under-ice community of smaller taxa. The Atlantic-influenced eastern region, with harsher high-light, low-nutrient conditions provided by earlier sea-ice melting under the influence of the northward flow of the WGC, harbored a low-diversity, highly specialized community dominated by larger centric diatoms and *Phaeocystis pouchetii*. The subspecies variability within *Micromonas polaris* and *Baffinella frigidus* species with distinct distribution patterns might indicate the existence of ecotypes with overlapping niches in ice-associated sites, while retaining the capacity to thrive in open waters. The distribution of *Pterosperma* sp. ASV_0244, *M. polaris* ASV_0154, *B. frigidus* sp. ASV_0041, and *Chrysochromulina* sp. ASV_0542, and their significant association with ice-covered sites in the present study indicate that these taxa might be good proxies for diversity changes related to sea-ice loss. The presence of taxa with intra-species variability such as *B. frigidus*, *M. arctica*, *Chaetoceros*, and *M. polaris* reinforces the urgency of renewed culturing efforts to better comprehend ecological limits. Although thinner sea ice could increase the magnitude of sub-ice blooms of taxa with a high carbon export potential such as *M. arctica* (Poulin et al., 2014) earlier in the season, our data indicate that as the Baffin Bay ice cover shrinks sooner and faster with an earlier spring bloom onset (Stroeve et al., 2014), widespread post-bloom conditions would be favored for longer periods of the growing season, leading to a community dominated by a much less diverse community for longer periods of the year.

Data accessibility statement

Physicochemical and biological data from the Green Edge project are available at http://www.obs-vlfr.fr/proof/php/GREENEDGE/x_datalist_1.php?xxop=greenedge&xcamp=amundsen and at <https://www.seanoe.org/data/00487/59892/> (Massicotte et al., 2019). Details can be found in Bruyant et al. (2022) and Massicotte et al. (2020). Raw metabarcoding sequences are available under the Accession Code PRJNA810033 from GenBank SRA. Source code for sequence processing and supplementary material is available at https://github.com/vaulot/Paper-2021-Vaulot-metapr2/tree/main/R_processing.

Supplemental files

The supplemental files for this article can be found as follows:

Supplemental material available in: https://github.com/catherine-gerikas/GE_Amundsen_18S_metaB_supplementary_material.

Acknowledgments

The authors wish to thank the officers and crew of CCGS *Amundsen*. The success of the field campaign was widely

attributed to G Bécu, J Lagunas, D Christiansen-Stowe, J Sansoulet, E Rehm, M Benot-Gagné, M-H Forget, and F Bruyant from Takuvik laboratory and J Bourdon, C Marec, and M Picheral from CNRS. They also thank Québec-Océan and the Polar Continental Shelf Program for their in-kind contribution in terms of polar logistics and scientific equipment. They thank the ABIMS platform of the FR2424 (CNRS, Sorbonne Université) for bioinformatics resources. They are very grateful to Margot Tragin for her help during sampling and onboard sample processing.

Funding

Catherine Gérikas Ribeiro was supported by the FONDECYT Project No. 3190827 and NatGeo Grant EC-99447R-23. The Green Edge project was funded by the following French and Canadian programs and agencies: ANR (Contract #111112), ArcticNet, CERC on Remote sensing of Canada's new Arctic frontier, CNES (project #131425), French Arctic Initiative, Fondation Total, CSA, LEFE, and IPEV (project #1164). Additional support was from the Natural Sciences and Engineering Research Council of Canada (NSERC) Discovery and Northern supplement grants (CL), the Fond de Recherche du Québec Nature et Technologies (FQRNT) (Québec Océan), and the Network of Centres of Excellence (Canada) ArcticNet. This project was conducted using the Canadian research icebreaker CCGS *Amundsen* with the support of the Amundsen Science program funded by the Canada Foundation for Innovation (CFI) Major Science Initiatives (MSI) Fund. The project was conducted under the scientific coordination of the Canada Excellence Research Chair on Remote sensing of Canada's new Arctic frontier and the CNRS & Université Laval Takuvik Joint International Laboratory (UMI3376). Nicole Trefault was supported by Fondecyt No. 1230758 and Millenium Nucleus MASH (NCN2021_033). DV was partially supported by the ANR Phenomap (ANR-20-CE02-0025).

Competing interests

The authors declare no competing financial interests.

Author contributions

CGR, ALS, DM, and DV processed the samples and produced data; CGR, DV, NT, CL, and ALS analyzed and interpreted data; All authors wrote, read, and approved the final manuscript.

References

- Alou-Font, E, Roy, S, Agustí, S, Gosselin, M. 2016. Cell viability, pigments and photosynthetic performance of Arctic phytoplankton in contrasting ice-covered and open-water conditions during the spring-summer transition. *Marine Ecology Progress Series* **543**: 89–106. DOI: <http://dx.doi.org/10.3354/meps11562>.
- Ardyna, M, Mundy, CJ, Mayot, N, Matthes, LC, Oziel, L, Horvat, C, Leu, E, Assmy, P, Hill, V, Matrai, PA, Gale, M, Melnikov, IA, Arrigo, KR. 2020. Under-ice phytoplankton blooms: Shedding light on the “invisible” part of Arctic primary production.

- Frontiers in Marine Science* **7**: 1–25. DOI: <http://dx.doi.org/10.3389/fmars.2020.608032>.
- Arrigo, KR, Perovich, DK, Pickart, RS, Brown, ZW, van Dijken, GL, Lowry, KE, Mills, MM, Palmer, MA, Balch, WM, Bahr, F, Bates, NR, Benitez-Nelson, C, Bowler, B, Brownlee, E, Ehn, JK, Frey, KE, Garley, R, Laney, SR, Lubelczyk, L, Mathis, J, Matsuoka, A, Mitchell, BG, Moore, GWK, Ortega-Retuerta, E, Pal, S, Polashenski, CM, Reynolds, RA, Schieber, B, Sosik, HM, Stephens, M, Swift, JH.** 2012. Massive phytoplankton blooms under Arctic sea ice. *Science* **336**: 1408. DOI: <http://dx.doi.org/10.1126/science.1215065>.
- Arrigo, KR, Perovich, DK, Pickart, RS, Brown, ZW, van Dijken, GL, Lowry, KE, Mills, MM, Palmer, MA, Balch, WM, Bates, NR, Benitez-Nelson, CR, Brownlee, E, Frey, KE, Laney, SR, Mathis, J, Matsuoka, A, Greg Mitchell, B, Moore, GW, Reynolds, RA, Sosik, HM, Swift, JH.** 2014. Phytoplankton blooms beneath the sea ice in the Chukchi sea. *Deep-Sea Research Part II: Topical Studies in Oceanography* **105**: 1–16. DOI: <http://dx.doi.org/10.1016/j.dsr2.2014.03.018>.
- Assmy, P, Fernández-Méndez, M, Duarte, P, Meyer, A, Randelhoff, A, Mundy, CJ, Olsen, LM, Kauko, HM, Bailey, A, Chierici, M, Cohen, L, Doulgeris, AP, Ehn, JK, Fransson, A, Gerland, S, Hop, H, Hudson, SR, Hughes, N, Itkin, P, Johnsen, G, King, JA, Koch, BP, Koenig, Z, Kwasniewski, S, Laney, SR, Nicolaus, M, Pavlov, AK, Polashenski, CM, Provost, C, Rösel, A, Sandbu, M, Spreen, G, Smedsrud, LH, Sundfjord, A, Taskjelle, T, Tatarek, A, Wiktor, J, Wagner, PM, Wold, A, Steen, H, Granskog, MA.** 2017. Leads in Arctic pack ice enable early phytoplankton blooms below snow-covered sea ice. *Scientific Reports* **7**: 1–9. DOI: <http://dx.doi.org/10.1038/srep40850>.
- Balzano, S, Marie, D, Gourvil, P, Vaultot, D.** 2012. Composition of the summer photosynthetic pico and nanoplankton communities in the Beaufort Sea assessed by T-RFLP and sequences of the 18S rRNA gene from flow cytometry sorted samples. *The ISME Journal* **6**(8): 1480–1498. DOI: <http://dx.doi.org/10.1038/ismej.2011.213>.
- Balzano, S, Percopo, I, Siano, R, Gourvil, P, Chanoine, M, Marie, D, Vaultot, D, Sarno, D.** 2017. Morphological and genetic diversity of Beaufort Sea diatoms with high contributions from the *Chaetoceros neogracilis* species complex. *Journal of Phycology* **53**(1): 161–187. DOI: <http://dx.doi.org/10.1111/jpy.12489>.
- Benner, I, Irwin, AJ, Finkel, Z.** 2019. Capacity of the common Arctic picoeukaryote *Micromonas* to adapt to a warming ocean. *Limnology and Oceanography Letters* **5**(2): 221–227. DOI: <http://dx.doi.org/10.1002/lol2.10133>.
- Bluhm, BA, Kosobokova, KN, Carmack, EC.** 2015. A tale of two basins: An integrated physical and biological perspective of the deep Arctic Ocean. *Progress in Oceanography* **139**: 89–121. DOI: <http://dx.doi.org/10.1016/j.pocean.2015.07.011>.
- Boetius, A, Albrecht, S, Bakker, K, Bienhold, C, Felden, J, Fernández-Méndez, M, Hendricks, S, Katlein, C, Lalande, C, Krumpfen, T, Nicolaus, M, Peeken, I, Rabe, B, Rogacheva, A, Rybakova, E, Somavilla, R, Wenzhöfer, F, Felden, J, RV Polarstern ARK27-3-Shipboard Science Party.** 2013. Export of algal biomass from the melting Arctic Sea ice. *Science* **339**(6126): 1430–1432. DOI: <http://dx.doi.org/10.1126/science.1231346>.
- Bruyant, F, Amiraux, R, Amyot, MP, Archambault, P, Artigue, L, Bardedo de Freitas, L, Bécu, G, Bélanger, S, Bourgain, P, Bricaud, A, Brouard, E, Brunet, C, Burgers, T, Caleb, D, Chalut, K, Clautre, H, Cornet-Barthaux, V, Coupel, P, Cusa, M, Cusset, F, Dadaglio, L, Davelaar, M, Deslongchamps, G, Dimier, C, Dinasquet, J, Dumont, D, Else, B, Eulaers, I, Ferland, J, Filteau, G, Forget, MH, Fort, J, Fortier, L, Galí-Tapías, M, Gallinari, M, Garbus, SE, Garcia, N, Gérikas Ribeiro, C, Gombault, C, Gourvil, P, Goyens, C, Grant, C, Grondin, PL, Guillot, P, Hillion, S, Hussher, R, Joux, F, Joy-Warren, H, Joyal, G, Kieber, D, Lafond, A, Lagunas, J, Lajeunesse, P, Lalande, C, Larivière, J, Le Gall, F, Leblanc, K, Leblanc, M, Legras, J, Levesque, K, Lewis, KM, Leymarie, E, Leynaert, A, Linkowski, T, Lizotte, M, Lopes dos Santos, A, Marec, C, Marie, D, Massé, G, Massicotte, P, Matsuoka, A, Miller, L, Mirshak, S, Morata, N, Moriceau, B, Morin, PI, Morisset, S, Mosbech, A, Mucci, A, Nadai, G, Nozais, C, Obernosterer, I, Paire, T, Panagiotopoulos, C, Parenteau, M, Pelletier, N, Picheral, M, Quéguiner, B, Raimbault, P, Ras, J, Rehm, E, Ribot Lacosta, L, Rontani, JF, Saint-Béat, B, Sansoulet, J, Sardet, N, Schmechtig, C, Sciandra, A, Sempéré, R, Sévigny, C, Toullec, J, Tragin, M, Tremblay, JE, Trottier, AP, Vaultot, D, Vladioiu, A, Xue, L, Yunda-Guarin, G, Babin, M.** 2022. The Green Edge cruise: Investigating the marginal ice zone processes during late spring and early summer to understand the fate of the Arctic phytoplankton bloom. *Earth System Science Data* **14**(10): 4607–4642. DOI: <http://dx.doi.org/10.5194/essd-14-4607-2022>.
- Burgers, TM, Tremblay, JÉ, Else, BGT, Papakyriakou, TN.** 2020. Estimates of net community production from multiple approaches surrounding the spring ice-edge bloom in Baffin Bay. *Elementa: Science of the Anthropocene* **8**(1): 013. DOI: <http://dx.doi.org/10.1525/elementa.013>.
- Callahan, BJ, McMurdie, PJ, Rosen, MJ, Han, AW, Johnson, AJA, Holmes, SP.** 2016. DADA2: High-resolution sample inference from Illumina amplicon data. *Nature Methods* **13**: 581–583. DOI: <http://dx.doi.org/10.1038/nmeth.3869>.
- Chang, FH, Sutherland, J, Bradford-Grieve, J.** 2017. Taxonomic revision of Dictyochaetales (Dictyochophyceae) based on morphological, ultrastructural, biochemical and molecular data. *Phycological Research* **65**(3):

- 235–247. DOI: <http://dx.doi.org/10.1111/pre.12181>.
- Comeau, AM, Philippe, B, Thaler, M, Gosselin, M, Poulin, M, Lovejoy, C.** 2013. Protists in Arctic drift and land-fast sea ice. *Journal of Phycology* **49**(2): 229–240. DOI: <http://dx.doi.org/10.1111/jpy.12026>.
- Crawford, DW, Cefarelli, AO, Wrohan, IA, Wyatt, SN, Varela, DE.** 2018. Spatial patterns in abundance, taxonomic composition and carbon biomass of nano- and microphytoplankton in Subarctic and Arctic Seas. *Progress in Oceanography* **162**: 132–159. DOI: <http://dx.doi.org/10.1016/j.pocean.2018.01.006>.
- Croteau, D, Lacour, T, Schiffrine, N, Morin, PI, Forget, MH, Bruyant, F, Ferland, J, Lafond, A, Campbell, DA, Tremblay, JÉ, Babin, M, Lavaud, J.** 2022. Shifts in growth light optima among diatom species support their succession during the spring bloom in the Arctic. *Journal of Ecology* **110**(6): 1356–1375. DOI: <http://dx.doi.org/10.1111/1365-2745.13874>.
- Daugbjerg, N, Norlin, A, Lovejoy, C.** 2018. *Baffinella frigidus* gen. et sp. nov. (Baffinellaceae fam. nov., Cryptophyceae) from Baffin Bay: Morphology, pigment profile, phylogeny, and growth rate response to three abiotic factors. *Journal of Phycology* **54**(5): 665–680. DOI: <http://dx.doi.org/10.1111/jpy.12766>.
- De Cáceres, M, Legendre, P, Moretti, M.** 2010. Improving indicator species analysis by combining groups of sites. *Oikos* **119**(10): 1674–1684. DOI: <http://dx.doi.org/10.1111/j.1600-0706.2010.18334.x>.
- Demory, D, Baudoux, AC, Monier, A, Simon, N, Six, C, Ge, P, Rigaut-Jalabert, F, Marie, D, Sciandra, A, Bernard, O, Rabouille, S.** 2019. Picoeukaryotes of the *Micromonas* genus: Sentinels of a warming ocean. *The ISME Journal* **13**(1): 132–146. DOI: <http://dx.doi.org/10.1038/s41396-018-0248-0>.
- Dixon, P.** 2003. Computer program review VEGAN, a package of R functions for community ecology. *Journal of Vegetation Science* **14**(6): 927–930. DOI: <http://dx.doi.org/10.1111/j.1654-1103.2003.tb02228.x>.
- Egge, ES, Eikrem, W, Edvardsen, B.** 2014. Deep-branching novel lineages and high diversity of Haptophytes in the Skagerrak (Norway) uncovered by 454 pyrosequencing. *The Journal of Eukaryotic Microbiology* **62**(1): 121–140. DOI: <http://dx.doi.org/10.1111/jeu.12157>.
- Freyria, NJ, Joli, N, Lovejoy, C.** 2021. A decadal perspective on north water microbial eukaryotes as Arctic Ocean sentinels. *Scientific Reports* **11**: 1–14. DOI: <http://dx.doi.org/10.1038/s41598-021-87906-4>.
- García-García, N, Tamames, J, Linz, AM, Pedrós-Alió, C, Puente-Sánchez, F.** 2019. Microdiversity ensures the maintenance of functional microbial communities under changing environmental conditions. *ISME Journal* **13**(12): 2969–2983. DOI: <http://dx.doi.org/10.1038/s41396-019-0487-8>.
- Godhe, A, Rynearson, T.** 2017. The role of intraspecific variation in the ecological and evolutionary success of diatoms in changing environments. *Philosophical Transactions of the Royal Society B: Biological Sciences* **372**(1728). DOI: <http://dx.doi.org/10.1098/rstb.2016.0399>.
- Goeyens, L, Kindermans, N, Abu Yusuf, M, Elskens, M.** 1998. A room temperature procedure for the manual determination of urea in seawater. *Estuarine, Coastal and Shelf Science* **47**(4): 415–418. DOI: <http://dx.doi.org/10.1006/ecss.1998.0357>.
- Guillou, L, Bachar, D, Audic, S, Bass, D, Berney, C, Bittner, L, Boutte, C, Burgaud, G, De Vargas, C, Decelle, J, Del Campo, J, Dolan, JR, Dunthorn, M, Edvardsen, B, Holzmann, M, Kooistra, WH, Lara, E, Le Bescot, N, Logares, R, Mahé, F, Massana, R, Montresor, M, Morard, R, Not, F, Pawlowski, J, Probert, I, Sauvadet, AL, Siano, R, Stoeck, T, Vaulot, D, Zimmermann, P, Christen, R.** 2013. The Protist Ribosomal Reference database (PR²): A catalog of unicellular eukaryote small sub-unit rRNA sequences with curated taxonomy. *Nucleic Acids Research* **41**(Database issue): D597–D604. DOI: <http://dx.doi.org/10.1093/nar/gks1160>.
- Hamilton, M, Mascioni, M, Hehenberger, E, Bachy, C, Yung, C, Vernet, M, Worden, AZ.** 2021. Spatiotemporal variations in Antarctic protistan communities highlight phytoplankton diversity and seasonal dominance by a novel cryptophyte lineage. *mBio* **12**(6): e02973-21. DOI: <http://dx.doi.org/10.1128/mBio.02973-21>.
- Hardge, K, Peeken, I, Neuhaus, S, Lange, BA, Stock, A, Stoeck, T, Weinisch, L, Metfies, K.** 2017. The importance of sea ice for exchange of habitat-specific protist communities in the central Arctic Ocean. *Journal of Marine Systems* **165**: 124–138. DOI: <http://dx.doi.org/10.1016/j.jmarsys.2016.10.004>.
- Hegseth, NE, Sundfjord, A.** 2008. Intrusion and blooming of Atlantic phytoplankton species in the high Arctic. *Journal of Marine Systems* **74**(1–2): 108–119. DOI: <http://dx.doi.org/10.1016/j.jmarsys.2007.11.011>.
- Hilligsøe, KM, Richardson, K, Bendtsen, J, Sørensen, LL, Nielsen, TG, Lyngsgaard, MM.** 2011. Linking phytoplankton community size composition with temperature, plankton food web structure and sea–air CO₂ flux. *Deep-Sea Research Part I: Oceanographic Research Papers* **58**(8): 826–838. DOI: <http://dx.doi.org/10.1016/j.dsr.2011.06.004>.
- Holmes, RM, Aminot, A, Kérouel, R, Hooker, BA, Peterson, BJ.** 1999. A simple and precise method for measuring ammonium in marine and freshwater ecosystems. *Canadian Journal of Fisheries and Aquatic Sciences* **56**(10): 1801–1808. DOI: <http://dx.doi.org/10.1139/cjfas-56-10-1801>.
- Hop, H, Mundy, CJ, Gosselin, M, Rossnagel, AL, Barber, DG.** 2011. Zooplankton boom and ice amphipod bust below melting sea ice in the Amundsen Gulf, Arctic Canada. *Polar Biology* **34**: 1947–1958. DOI: <http://dx.doi.org/10.1007/s00300-011-0991-4>.
- Hop, H, Vihtakari, M, Bluhm, BA, Assmy, P, Poulin, M, Gradinger, R, Peeken, I, von Quillfeldt, C, Olsen,**

- LM, Zhitina, L, Melnikov, IA.** 2020. Changes in sea-ice protist diversity with declining sea ice in the Arctic Ocean from the 1980s to 2010s. *Frontiers in Marine Science* **7**. DOI: <http://dx.doi.org/10.3389/fmars.2020.00243>.
- Hoppe, CJM, Flintrop, CM, Rost, B.** 2018. The Arctic picoeukaryote *Micromonas pusilla* benefits synergistically from warming and ocean acidification. *Biogeosciences* **15**(14): 4353–4365. DOI: <http://dx.doi.org/10.5194/bg-15-4353-2018>.
- Horvat, C, Jones, DR, Iams, S, Schroeder, D, Flocco, D, Feltham, D.** 2017. The frequency and extent of sub-ice phytoplankton blooms in the Arctic Ocean. *Science Advances* **3**(3): e1601191. DOI: <http://dx.doi.org/10.1126/sciadv.1601191>.
- Ibarbalz, FM, Henry, N, Mahé, F, Ardyna, M, Zingone, A, Scalco, E, Lovejoy, C, Lombard, F, Jaillon, O, Iudicone, D, Malviya, S, Sullivan, MB, Chaffron, S, Karsenti, E, Babin, M, Boss, E, Wincker, P, Zinger, L, de Vargas, C, Bowler, C, Karp-Boss, L.** 2023. Pan-Arctic plankton community structure and its global connectivity. *Elementa: Science of the Anthropocene* **11**(1): 00060. DOI: <http://dx.doi.org/10.1525/elementa.2022.00060>.
- Jacquemot, L, Vigneron, A, Tremblay, JÉ, Lovejoy, C.** 2022. Contrasting sea ice conditions shape microbial food webs in Hudson Bay (Canadian Arctic). *ISME Communications* **2**: 1–10. DOI: <http://dx.doi.org/10.1038/s43705-022-00192-7>.
- Janout, MA, Hölemann, J, Waite, AM, Krumpfen, T, von Appen, WJ, Martynov, F.** 2016. Sea-ice retreat controls timing of summer plankton blooms in the Eastern Arctic Ocean. *Geophysical Research Letters* **43**(24): 12493–12501. DOI: <http://dx.doi.org/10.1002/2016GL071232>.
- Joli, N, Monier, A, Logares, R, Lovejoy, C.** 2017. Seasonal patterns in Arctic prasinophytes and inferred ecology of *Bathycoccus* unveiled in an Arctic winter metagenome. *ISME Journal* **11**(6): 1372–1385. DOI: <http://dx.doi.org/10.1038/ismej.2017.7>.
- Jones, EP, Swift, JH, Anderson, LG, Lipizer, M, Civitarese, G, Falkner, KK, Kattner, G, McLaughlin, F.** 2003. Tracing Pacific water in the North Atlantic Ocean. *Journal of Geophysical Research C: Oceans* **108**(C4). DOI: <http://dx.doi.org/10.1029/2001jc001141>.
- Joy-Warren, HL, Lewis, KM, Ardyna, M, Tremblay, JÉ, Babin, M, Arrigo, KR.** 2023. Similarity in phytoplankton photophysiology among under-ice, marginal ice, and open water environments of Baffin Bay (Arctic Ocean). *Elementa: Science of the Anthropocene* **11**(1): 00080. DOI: <http://dx.doi.org/10.1525/elementa.2021.00080>.
- Kalenitchenko, D, Joli, N, Potvin, M, Tremblay, JÉ, Lovejoy, C.** 2019. Biodiversity and species change in the Arctic Ocean: A view through the lens of Nares Strait. *Frontiers in Marine Science* **6**: 1–17. DOI: <http://dx.doi.org/10.3389/fmars.2019.00479>.
- Kauko, HM, Olsen, LM, Duarte, P, Peeken, I, Granskog, MA, Johnsen, G, Fernández-Méndez, M, Pavlov, AK, Mundy, CJ, Assmy, P.** 2018. Algal colonization of young Arctic sea ice in spring. *Frontiers in Marine Science* **5**: 1–20. DOI: <http://dx.doi.org/10.3389/fmars.2018.00199>.
- Kinney, JC, Maslowski, W, Osinski, R, Jin, M, Frants, M, Jeffery, N, Lee, YJ.** 2020. Hidden production: On the importance of pelagic phytoplankton blooms beneath Arctic sea ice. *Journal of Geophysical Research: Oceans* **125**(9): e2020JC016211. DOI: <http://dx.doi.org/10.1029/2020JC016211>.
- Kvernvik, AC, Rokitta, SD, Leu, E, Harms, L, Gabrielsen, TM, Rost, B, Hoppe, CJM.** 2020. Higher sensitivity towards light stress and ocean acidification in an Arctic sea-ice-associated diatom compared to a pelagic diatom. *New Phytologist* **226**(6): 1708–1724. DOI: <http://dx.doi.org/10.1111/nph.16501>.
- Lafond, A, Leblanc, K, Quéguiner, B, Moriceau, B, Leynaert, A, Cornet, V, Legras, J, Ras, J, Parenteau, M, Garcia, N, Babin, M, Tremblay, JÉ.** 2019. Late spring bloom development of pelagic diatoms in Baffin Bay. *Elementa: Science of the Anthropocene* **7**: 44. DOI: <http://dx.doi.org/10.1525/elementa.382>.
- Lalande, C, Bauerfeind, E, Nöthig, EM, Beszczynska-Möller, A.** 2013. Impact of a warm anomaly on export fluxes of biogenic matter in the eastern Fram Strait. *Progress in Oceanography* **109**: 70–77. DOI: <http://dx.doi.org/10.1016/j.pocean.2012.09.006>.
- Lasternas, S, Agust, S.** 2010. Phytoplankton community structure during the record Arctic ice-melting of summer 2007. *Polar Biology* **33**: 1709–1717. DOI: <http://dx.doi.org/10.1007/s00300-010-0877-x>.
- Leu, E, Mundy, CJ, Assmy, P, Campbell, K, Gabrielsen, TM, Gosselin, M, Juul-Pedersen, T, Gradinger, R.** 2015. Arctic spring awakening—Steering principles behind the phenology of vernal ice algal blooms. *Progress in Oceanography* **139**: 151–170. DOI: <http://dx.doi.org/10.1016/j.pocean.2015.07.012>.
- Leu, E, Søreide, JE, Hessen, DO, Falk-Petersen, S, Berge, J.** 2011. Consequences of changing sea-ice cover for primary and secondary producers in the European Arctic shelf seas: Timing, quantity, and quality. *Progress in Oceanography* **90**(1–4): 18–32. DOI: <http://dx.doi.org/10.1016/j.pocean.2011.02.004>.
- Lewis, KM, Arntsen, AE, Coupel, P, Joy-Warren, H, Lowry, KE, Matsuoka, A, Mills, MM, van Dijken, GL, Selz, V, Arrigo, KR.** 2019. Photoacclimation of Arctic Ocean phytoplankton to shifting light and nutrient limitation. *Limnology and Oceanography* **64**(1): 284–301. DOI: <http://dx.doi.org/10.1002/lno.11039>.
- Li, WK, McLaughlin, FA, Lovejoy, C, Carmack, EC.** 2009. Smallest algae thrive as the Arctic Ocean freshens. *Science* **326**(5932): 539. DOI: <http://dx.doi.org/10.1126/science.1179798>.
- Lin, Y, Moreno, C, Marchetti, A, Ducklow, H, Schofield, O, Delage, E, Meredith, M, Li, Z, Eveillard, D, Chaffron, S, Cassar, N.** 2021. Decline in plankton diversity and carbon flux with reduced sea ice extent

- along the Western Antarctic Peninsula. *Nature Communications* **12**: 1–9. DOI: <http://dx.doi.org/10.1038/s41467-021-25235-w>.
- Lovejoy, C, Legendre, L, Martineau, MJ, Bâcle, J, von Quillfeldt, CH.** 2002. Distribution of phytoplankton and other protists in the North Water. *Deep-Sea Research Part II: Topical Studies in Oceanography* **49**(22–23): 5027–5047. DOI: [http://dx.doi.org/10.1016/S0967-0645\(02\)00176-5](http://dx.doi.org/10.1016/S0967-0645(02)00176-5).
- Lovejoy, C, Potvin, M.** 2011. Microbial eukaryotic distribution in a dynamic Beaufort Sea and the Arctic Ocean. *Journal of Plankton Research* **33**(3): 431–444. DOI: <http://dx.doi.org/10.1093/plankt/fbq124>.
- Lovejoy, C, Vincent, WF, Bonilla, S, Roy, S, Martineau, MJ, Terrado, R, Potvin, M, Massana, R, Pedrós-Alió, C.** 2007. Distribution, phylogeny, and growth of cold-adapted picoprasinophytes in Arctic seas. *Journal of Phycology* **43**(1): 78–89. DOI: <http://dx.doi.org/10.1111/j.1529-8817.2006.00310.x>.
- Luo, W, Li, H, Gao, S, Yu, Y, Lin, L, Zeng, Y.** 2016. Molecular diversity of microbial eukaryotes in sea water from Fildes Peninsula, King George Island, Antarctica. *Polar Biology* **39**: 605–616. DOI: <http://dx.doi.org/10.1007/s00300-015-1815-8>.
- Marie, D, Partensky, F, Jacquet, S, Vaultot, D.** 1997. Enumeration and cell cycle analysis of natural populations of marine picoplankton by flow cytometry using the nucleic acid stain SYBR Green I. *Applied and Environmental Microbiology* **63**(1): 186–193. DOI: <http://dx.doi.org/10.1128/aem.63.1.186-193.1997>.
- Marie, D, Shi, XL, Rigaut-Jalabert, F, Vaultot, D.** 2010. Use of flow cytometric sorting to better assess the diversity of small photosynthetic eukaryotes in the English Channel. *FEMS Microbiology Ecology* **72**(2): 165–178. DOI: <http://dx.doi.org/10.1111/j.1574-6941.2010.00842.x>.
- Martin, J, Tremblay, JÉ, Gagnon, J, Tremblay, G, Lapoussière, A, Jose, C, Poulin, M, Gosselin, M, Gratton, Y, Michel, C.** 2010. Prevalence, structure and properties of subsurface chlorophyll maxima in Canadian Arctic waters. *Marine Ecology Progress Series* **412**: 69–84. DOI: <http://dx.doi.org/10.3354/meps08666>.
- Massicotte, P, Amiraux, R, Amyot, MP, Archambault, P, Ardyna, M, Arnaud, L, Artigue, L, Aubry, C, Ayotte, P, Bécu, G, Bélanger, S, Benner, R, Bittig, HC, Bricaud, A, Brossier, É, Bruyant, F, Chauvaud, L, Christiansen-Stowe, D, Claustre, H, Cornet-Barthaux, V, Coupel, P, Cox, C, Delaforge, A, Dezutter, T, Dimier, C, Domine, F, Dufour, F, Dufresne, C, Dumont, D, Ehn, J, Else, B, Ferland, J, Forget, MH, Fortier, L, Gal, M, Galindo, V, Gallinari, M, Garcia, N, Gérikas Ribeiro, C, Gourdal, M, Gourvil, P, Goyens, C, Grondin, PL, Guillot, P, Guilmette, C, Houssais, MN, Joux, F, Lacour, L, Lacour, T, Lafond, A, Lagunas, J, Lalande, C, Laliberté, J, Lambert-Girard, S, Larivière, J, Lavaud, J, LeBaron, A, Leblanc, K, Le Gall, F, Legras, J, Lemire, M, Levasseur, M, Leymarie, E, Leynaert, A, Lopes dos Santos, A, Lourenço, A, Mah, D, Marec, C, Marie, D, Martin, N, Marty, C, Marty, S, Massé, G, Matsuoka, A, Matthes, L, Moriceau, B, Muller, PE, Mundy, CJ, Neukermans, G, Oziel, L, Panagiotopoulos, C, Pangrazi, JJ, Picard, G, Picheral, M, Pinczon du Sel, F, Pogorzelec, N, Probert, I, Quéguiner, B, Raimbault, P, Ras, J, Rehm, E, Reimer, E, Rontani, JF, Rysgaard, S, Saint-Béat, B, Sampei, M, Sansoulet, J, Schmechtig, C, Schmidt, S, Sempéré, R, Sévigny, C, Shen, Y, Tragin, M, Tremblay, JÉ, Vaultot, D, Verin, G, Vivier, F, Vladioiu, A, Whitehead, J, Babin, M.** 2019. Green Edge initiative: Understanding the processes controlling the under-ice Arctic phytoplankton spring bloom. *SEANOE*. DOI: <http://dx.doi.org/10.17882/59892>.
- Massicotte, P, Amiraux, R, Amyot, MP, Archambault, P, Ardyna, M, Arnaud, L, Artigue, L, Aubry, C, Ayotte, P, Bécu, G, Bélanger, S, Benner, R, Bittig, HC, Bricaud, A, Brossier, É, Bruyant, F, Chauvaud, L, Christiansen-Stowe, D, Claustre, H, Cornet-Barthaux, V, Coupel, P, Cox, C, Delaforge, A, Dezutter, T, Dimier, C, Domine, F, Dufour, F, Dufresne, C, Dumont, D, Ehn, J, Else, B, Ferland, J, Forget, MH, Fortier, L, Gal, M, Galindo, V, Gallinari, M, Garcia, N, Gérikas Ribeiro, C, Gourdal, M, Gourvil, P, Goyens, C, Grondin, PL, Guillot, P, Guilmette, C, Houssais, MN, Joux, F, Lacour, L, Lacour, T, Lafond, A, Lagunas, J, Lalande, C, Laliberté, J, Lambert-Girard, S, Larivière, J, Lavaud, J, LeBaron, A, Leblanc, K, Le Gall, F, Legras, J, Lemire, M, Levasseur, M, Leymarie, E, Leynaert, A, Lopes dos Santos, A, Lourenço, A, Mah, D, Marec, C, Marie, D, Martin, N, Marty, C, Marty, S, Massé, G, Matsuoka, A, Matthes, L, Moriceau, B, Muller, PE, Mundy, CJ, Neukermans, G, Oziel, L, Panagiotopoulos, C, Pangrazi, JJ, Picard, G, Picheral, M, Pinczon du Sel, F, Pogorzelec, N, Probert, I, Quéguiner, B, Raimbault, P, Ras, J, Rehm, E, Reimer, E, Rontani, JF, Rysgaard, S, Saint-Béat, B, Sampei, M, Sansoulet, J, Schmechtig, C, Schmidt, S, Sempéré, R, Sévigny, C, Shen, Y, Tragin, M, Tremblay, JÉ, Vaultot, D, Verin, G, Vivier, F, Vladioiu, A, Whitehead, J, Babin, M.** 2020. Green Edge ice camp campaigns: Understanding the processes controlling the under-ice Arctic phytoplankton spring bloom. *Earth System Science Data* **12**(1): 151–176. DOI: <http://dx.doi.org/10.5194/essd-12-151-2020>.
- Matsuoka, A, Larouche, P, Poulin, M, Vincent, W, Hattori, H.** 2009. Phytoplankton community adaptation to changing light levels in the southern Beaufort Sea, Canadian Arctic. *Estuarine, Coastal and Shelf Science* **82**(3): 537–546. DOI: <http://dx.doi.org/10.1016/j.ecss.2009.02.024>.
- McMurdie, PJ, Holmes, S.** 2013. Phyloseq: An R package for reproducible interactive analysis and graphics of microbiome census data. *PLoS One* **8**. DOI: <http://dx.doi.org/10.1371/journal.pone.0061217>.

- Meredith, M, Sommerkorn, M, Cassotta, S, Derksen, C, Ekaykin, A, Hollowed, A, Kofinas, G, Mackintosh, A, Melbourne-Thomas, J, Muelbert, M, Ottersen, G, Pritchard, H, Schuur, E.** 2019. Polar regions, in Pörtner, HO, Roberts, D, Masson-Delmotte, V, Zhai, P, Tignor, M, Poloczanska, E, Mintenbeck, K, Alegría, A, Nicolai, M, Okem, A, Petzold, J, Rama, B, Weyer, N eds., *IPCC special report on the ocean and cryosphere in a changing climate*. New York, NY: Cambridge University Press: 203–320. DOI: <https://doi.org/10.1017/9781009157964.005>.
- Metfies, K, Von Appen, WJ, Kiliyas, E, Nicolaus, A, Nöthig, EM.** 2016. Biogeography and photosynthetic biomass of Arctic marine pico-eukaryotes during summer of the record sea ice minimum 2012. *PLoS One* **11**: 1–20. DOI: <http://dx.doi.org/10.1371/journal.pone.0148512>.
- Moestrup, Ø, Thomsen, H.** 1990. *Dictyocha speculum* (Silicoflagellata, Dictyochophyceae). Studies on armoured and unarmoured stages. *Biologiske skrifter/Det Kongelige Danske Videnskabernes Selskab* **37**: 1–56.
- Morán, XAG, López-Urrutia, Á, Calvo-Díaz, A, Li, WK.** 2010. Increasing importance of small phytoplankton in a warmer ocean. *Global Change Biology* **16**(3): 1137–1144. DOI: <http://dx.doi.org/10.1111/j.1365-2486.2009.01960.x>.
- Morando, M, Capone, DG.** 2018. Direct utilization of organic nitrogen by phytoplankton and its role in nitrogen cycling within the Southern California Bight. *Frontiers in Microbiology* **9**: 1–13. DOI: <http://dx.doi.org/10.3389/fmicb.2018.02118>.
- Münchow, A, Falkner, KK, Melling, H.** 2015. Baffin Island and West Greenland current systems in northern Baffin Bay. *Progress in Oceanography* **132**: 305–317. DOI: <http://dx.doi.org/10.1016/j.pocean.2014.04.001>.
- Mundy, CJ, Gosselin, M, Ehn, JK, Belzile, C, Poulin, M, Alou, E, Roy, S, Hop, H, Lessard, S, Papakyriakou, TN, Barber, DG, Stewart, J.** 2011. Characteristics of two distinct high-light acclimated algal communities during advanced stages of sea ice melt. *Polar Biology* **34**: 1869–1886. DOI: <http://dx.doi.org/10.1007/s00300-011-0998-x>.
- Needham, DM, Fuhrman, JA.** 2016. Pronounced daily succession of phytoplankton, archaea and bacteria following a spring bloom. *Nature Microbiology* **1**: 1–7. DOI: <http://dx.doi.org/10.1038/nmicrobiol.2016.5>.
- Neukermans, G, Oziel, L, Babin, M.** 2018. Increased intrusion of warming Atlantic waters leads to rapid expansion of temperate phytoplankton in the Arctic. *Global Change Biology* **24**(6): 2545–2553. DOI: <http://dx.doi.org/10.1111/gcb.14075>.
- Newton, R, Schlosser, P, Mortlock, R, Swift, J, MacDonald, R.** 2013. Canadian Basin freshwater sources and changes: Results from the 2005 Arctic Ocean Section. *Journal of Geophysical Research: Oceans* **118**(4): 2133–2154. DOI: <http://dx.doi.org/10.1002/jgrc.20101>.
- Niemi, A, Michel, C, Hille, K, Poulin, M.** 2011. Protist assemblages in winter sea ice: Setting the stage for the spring ice algal bloom. *Polar Biology* **34**: 1803–1817. DOI: <http://dx.doi.org/10.1007/s00300-011-1059-1>.
- Not, F, Massana, R, Latasa, M, Marie, D, Pedro, C, Vaulot, D, Simon, N.** 2005. Late summer community composition and abundance of photosynthetic picoeukaryotes in Norwegian and Barents Seas. *Limnology and Oceanography* **50**(5): 1677–1686. DOI: <http://dx.doi.org/10.4319/lo.2005.50.5.1677>.
- Olsen, LM, Laney, SR, Duarte, P, Kauko, HM, Fernández-méndez, M, Mundy, CJ, Rösel, A, Meyer, A, Itkin, P, Cohen, L, Peeken, I, Tatarek, A, Róžańska-Pluta, M, Wiktor, J, Taskjelle, T, Pavlov, AK, Hudson, SR, Granskog, MA, Hop, H, Assmy, P.** 2017. The seeding of ice algal blooms in Arctic pack ice: The multiyear ice seed repository hypothesis. *Journal of Geophysical Research: Biogeosciences* **122**(7): 1529–1548. DOI: <http://dx.doi.org/10.1002/2016JG003668>.
- Oziel, L, Baudena, A, Ardyna, M, Massicotte, P, Randelhoff, A, Sallée, JB, Ingvaldsen, RB, Devred, E, Babin, M.** 2020. Faster Atlantic currents drive poleward expansion of temperate phytoplankton in the Arctic Ocean. *Nature Communications* **11**. DOI: <http://dx.doi.org/10.1038/s41467-020-15485-5>.
- Oziel, L, Massicotte, P, Randelhoff, A, Ferland, J, Vladoiu, A, Lacour, L, Galindo, V, Lambert-Girard, S, Dumont, D, Cuypers, Y, Bouruet-Aubertot, P, Mundy, CJ, Ehn, J, Bécu, G, Marec, C, Forget, MH, Garcia, N, Coupel, P, Raimbault, P, Houssais, MN, Babin, M.** 2019. Environmental factors influencing the seasonal dynamics of spring algal blooms in and beneath sea ice in western Baffin Bay. *Elementa: Science of the Anthropocene* **7**: 34. DOI: <http://dx.doi.org/10.1525/elementa.372>.
- Perrette, M, Yool, A, Quartly, GD, Popova, EE.** 2011. Near-ubiquity of ice-edge blooms in the Arctic. *Biogeosciences* **8**(2): 515–524. DOI: <http://dx.doi.org/10.5194/bg-8-515-2011>.
- Piredda, R, Tomasino, MP, D'Erchia, AM, Manzari, C, Pesole, G, Montresor, M, Kooistra, WH, Sarno, D, Zingone, A.** 2017. Diversity and temporal patterns of planktonic protist assemblages at a Mediterranean Long Term Ecological Research site. *FEMS Microbiology Ecology* **93**(1): fiw200. DOI: <http://dx.doi.org/10.1093/femsec/fiw200>.
- Piwosz, K, Wiktor, JM, Niemi, A, Tatarek, A, Michel, C.** 2013. Mesoscale distribution and functional diversity of picoeukaryotes in the first-year sea ice of the Canadian Arctic. *ISME Journal* **7**(8): 1461–1471. DOI: <http://dx.doi.org/10.1038/ismej.2013.39>.
- Polyakov, IV, Pnyushkov, AV, Alkire, MB, Ashik, IM, Baumann, TM, Carmack, EC, Goszczko, I, Guthrie, J, Ivanov, VV, Kanzow, T, Krishfield, R, Kwok, R, Sundfjord, A, Morison, J, Rember, R, Yulin, A.** 2017. Greater role for Atlantic inflows on sea-ice loss in the Eurasian Basin of the Arctic Ocean.

- Science* **356**(6335): 285–291. DOI: <http://dx.doi.org/10.1126/science.aai8204>.
- Post, E, Bhatt, US, Bitz, CM, Brodie, JF, Fulton, TL, Hebblewhite, M, Kerby, J, Kutz, SJ, Stirling, I, Walker, DA.** 2013. Ecological consequences of sea-ice decline. *Science* **341**(6145): 519–524. DOI: <http://dx.doi.org/10.1126/science.1235225>.
- Poulin, M, Underwood, GJ, Michel, C.** 2014. Sub-ice colonial *Melosira arctica* in Arctic first-year ice. *Diatom Research* **29**(2): 213–221. DOI: <http://dx.doi.org/10.1080/0269249X.2013.877085>.
- R Core Team.** 2021. *R: A language and environment for statistical computing*. Vienna, Austria: R Foundation for Statistical Computing. Available at <https://www.R-project.org/>. Accessed January 3, 2021.
- Randelhoff, A, Oziel, L, Massicotte, P, Bécu, G, Lacour, L, Dumont, D, Vladioiu, A, Marec, C, Bruyant, F, Houssais, MN, Tremblay, JÉ, Deslongchamps, G, Babin, M.** 2019. The evolution of light and vertical mixing across a phytoplankton ice-edge bloom. *Elementa: Science of the Anthropocene* **7**: 20. DOI: <http://dx.doi.org/10.1525/elementa.357>.
- Renaut, S, Devred, E, Babin, M.** 2018. Northward expansion and intensification of phytoplankton growth during the early ice-free season in Arctic. *Geophysical Research Letters* **45**(19): 10590–10598. DOI: <http://dx.doi.org/10.1029/2018GL078995>.
- Ribeiro, CG, Lopes, A, Gourvil, P, Gall, FL, Marie, D, Tragin, M, Probert, I, Vault, D.** 2020. Culturable diversity of Arctic phytoplankton during pack ice melting. *Elementa: Science of the Anthropocene* **8**: 6. DOI: <http://dx.doi.org/10.1525/elementa.401>.
- Ribeiro, CG, Lopes dos Santos, A, Marie, D, Helena Pellizari, V, Pereira Brandini, F, Vault, D.** 2016. Pico and nanoplankton abundance and carbon stocks along the Brazilian Bight. *PeerJ* **4**: e2587. DOI: <http://dx.doi.org/10.7717/peerj.2587>.
- Saint-Béat, B, Fath, BD, Aubry, C, Colombet, J, Dinasquet, J, Fortier, L, Galindo, V, Grondin, PL, Joux, F, Lalande, C, LeBlanc, M, Raimbault, P, Sime- Ngando, T, Tremblay, JE, Vault, D, Maps, F, Babin, M.** 2020. Contrasting pelagic ecosystem functioning in eastern and western Baffin Bay revealed by trophic network modeling. *Elementa: Science of the Anthropocene* **8**: 1. DOI: <http://dx.doi.org/10.1525/elementa.397>.
- Sakshaug, E.** 2004. Primary and secondary production in the Arctic seas, in Stein, R, MacDonald, R eds., *The organic carbon cycle in the Arctic Ocean*. Berlin, Germany: Heidelberg Springer: 57–81. DOI: http://dx.doi.org/10.1007/978-3-642-18912-8_3.
- Schiffrine, N, Tremblay, JÉ, Babin, M.** 2020. Growth and elemental stoichiometry of the ecologically-relevant Arctic diatom *Chaetoceros gelidus*: A mix of polar and temperate. *Frontiers in Marine Science* **6**: 1–15. DOI: <http://dx.doi.org/10.3389/fmars.2019.00790>.
- Schmidt, K, Brown, T, Belt, S, Ireland, L, Taylor, KW, Thorpe, S, Ward, P, Atkinson, A.** 2018. Do pelagic grazers benefit from sea ice? Insights from the Antarctic sea ice proxy IPSO₂₅. *Biogeosciences* **15**(7): 1987–2006. DOI: <http://dx.doi.org/10.5194/bg-15-1987-2018>.
- Schoemann, V, Becquevort, S, Stefels, J, Rousseau, V, Lancelot, C.** 2005. *Phaeocystis* blooms in the global ocean and their controlling mechanisms: A review. *Journal of Sea Research* **53**(1–2): 43–66. DOI: <http://dx.doi.org/10.1016/j.seares.2004.01.008>.
- Serreze, MC, Holland, MM, Stroeve, J.** 2007. Perspectives on the Arctic's shrinking sea-ice cover. *Science* **315**(5818): 1533–1536. DOI: <http://dx.doi.org/10.1126/science.1139426>.
- Simon, N, Foulon, E, Grulois, D, Six, C, Desdevises, Y, Latimier, M, Le Gall, F, Tragin, M, Houdan, A, Derelle, E, Jouenne, F, Marie, D, Le Panse, S, Vault, D, Marin, B.** 2017. Revision of the genus *Micromonas* Manton et Parke (Chlorophyta, Mamiellophyceae), of the type species *M. pusilla* (Butcher) Manton & Parke and of the species *M. commoda* van Baren, Bachy and Worden and description of two new species based on the genetic and phenotypic characterization of cultured isolates. *Protist* **168**(5): 612–635. DOI: <http://dx.doi.org/10.1016/j.jprotis.2017.09.002>.
- Sjöqvist, CO, Kremp, A.** 2016. Genetic diversity affects ecological performance and stress response of marine diatom populations. *ISME Journal* **10**(11): 2755–2766. DOI: <http://dx.doi.org/10.1038/ismej.2016.44>.
- Smyth, TJ, Tyrell, T, Tarrant, B.** 2004. Time series of coccolithophore activity in the Barents Sea, from twenty years of satellite imagery. *Geophysical Research Letters* **31**(11): 2–5. DOI: <http://dx.doi.org/10.1029/2004GL019735>.
- Stoeck, T, Bass, D, Nebel, M, Christen, R, Jones, MD, Breiner, HW, Richards, TA.** 2010. Multiple marker parallel tag environmental DNA sequencing reveals a highly complex eukaryotic community in marine anoxic water. *Molecular Ecology* **19**(s1): 21–31. DOI: <http://dx.doi.org/10.1111/j.1365-294X.2009.04480.x>.
- Stroeve, J, Markus, T, Boisvert, L, Miller, J, Barret, A.** 2014. Changes in Arctic melt season and implications for sea ice loss. *Geophysical Research Letters* **41**(4): 1216–1225. DOI: <http://dx.doi.org/10.1002/2013GL058951>.
- Tang, CC, Ross, CK, Yao, T, Petrie, B, DeTracey, BM, Dunlap, E.** 2004. The circulation, water masses and sea-ice of Baffin Bay. *Progress in Oceanography* **63**(4): 183–228. DOI: <http://dx.doi.org/10.1016/j.pcean.2004.09.005>.
- Tedesco, L, Vichi, M, Scoccimarro, E.** 2019. Sea-ice algal phenology in a warmer Arctic. *Science Advances* **5**(5). DOI: <http://dx.doi.org/10.1126/sciadv.aav4830>.
- Terrado, R, Scarcella, K, Thaler, M, Vincent, WF, Lovejoy, C.** 2013. Small phytoplankton in Arctic seas: Vulnerability to climate change. *Biodiversity* **14**(1): 2–18.

- Toullec, J, Moriceau, B, Vincent, D, Guidi, L, Lafond, A, Babin, M.** 2021. Processes controlling aggregate formation and distribution during the Arctic phytoplankton spring bloom in Baffin Bay. *Elementa: Science of the Anthropocene* **9**(1): 00001. DOI: <http://dx.doi.org/10.1525/elementa.2021.00001>.
- Tragin, M, Vaulot, D.** 2019. Novel diversity within marine Mamiellophyceae (Chlorophyta) unveiled by metabarcoding. *Scientific Reports* **9**: 1–14. DOI: <http://dx.doi.org/10.1038/s41598-019-41680-6>.
- Trefault, N, De la Iglesia, R, Moreno-Pino, M, Lopes dos Santos, A, G erikas Ribeiro, C, Parada-Pozo, G, Cristi, A, Marie, D, Vaulot, D.** 2021. Annual phytoplankton dynamics in coastal waters from Fildes Bay, Western Antarctic Peninsula. *Scientific Reports* **11**: 1–16. DOI: <http://dx.doi.org/10.1038/s41598-020-80568-8>.
- Vader, A, Marquardt, M, Meshram, AR, Gabrielsen, TM.** 2015. Key Arctic phototrophs are widespread in the polar night. *Polar Biology* **38**: 13–21. DOI: <http://dx.doi.org/10.1007/s00300-014-1570-2>.
- Vaulot, D, Sim, CWH, Ong, D, Teo, B, Biwer, C, Jamy, M, Lopes dos Santos, A.** 2022. MetaPR²: A database of eukaryotic 18S rRNA metabarcodes with an emphasis on protists. *Molecular Ecology Resources* **22**(8): 3188–3201. DOI: <http://dx.doi.org/10.1111/1755-0998.13674>.
- Verity, PG, Brussaard, CP, Nejstgaard, JC, Van Leeuwe, MA, Lancelot, C, Medlin, LK.** 2007. Current understanding of *Phaeocystis* ecology and biogeochemistry, and perspectives for future research, in van Leeuwe, MA, Stefels, J, Belviso, S, Lancelot, C, Verity, PG, Gieskes, WWC eds., *Phaeocystis, major link in the biogeochemical cycling of climate-relevant elements*. Dordrecht, the Netherlands: Springer: 311–330. DOI: http://dx.doi.org/10.1007/978-1-4020-6214-8_21.
- Vilgrain, L, Maps, F, Picheral, M, Babin, M, Aubry, C, Irisson, JO, Ayata, SD.** 2021. Trait-based approach using in situ copepod images reveals contrasting ecological patterns across an Arctic ice melt zone. *Limnology and Oceanography* **66**(4): 1155–1167. DOI: <http://dx.doi.org/10.1002/lno.11672>.
- Wassmann, P, Reigstad, M, Haug, T, Rudels, B, Carroll, ML, Hop, H, Gabrielsen, GW, Falk-Petersen, S, Denisenko, SG, Arashkevich, E, Slagstad, D, Pavlova, O.** 2006. Food webs and carbon flux in the Barents Sea. *Progress in Oceanography* **71**(2–4): 232–287. DOI: <http://dx.doi.org/10.1016/j.pocean.2006.10.003>.
- Wickham, H.** 2016. *ggplot2: Elegant graphics for data analysis*. New York, NY: Springer-Verlag. DOI: <https://dx.doi.org/10.1007/978-0-387-98141-3>.
- Wickham, H, Averick, M, Bryan, J, Chang, W, McGowan, LD, Fran ois, R, Grolemund, G, Hayes, A, Henry, L, Hester, J, Kuhn, M, Pedersen, TL, Miller, E, Bache, SM, M uller, K, Ooms, J, Robinson, D, Seidel, DP, Spinu, V, Takahashi, K, Vaughan, D, Wilke, C, Woo, K, Yutani, H.** 2019. Welcome to the Tidyverse. *Journal of Open Source Software* **4**(43): 1686. DOI: <http://dx.doi.org/10.21105/joss.01686>.
- Xu, D, Kong, H, Yang, EJ, Li, X, Jiao, N, Warren, A, Wang, Y, Lee, Y, Jung, J, Kang, SH.** 2020. Contrasting community composition of active microbial eukaryotes in melt ponds and sea water of the Arctic Ocean revealed by high throughput sequencing. *Frontiers in Microbiology* **11**: 1–15. DOI: <http://dx.doi.org/10.3389/fmicb.2020.01170>.
- Zweng, MM, M unchow, A.** 2006. Warming and freshening of Baffin Bay, 1916–2003. *Journal of Geophysical Research: Oceans* **111**(C7): 1–13. DOI: <http://dx.doi.org/10.1029/2005JC003093>.

How to cite this article: Ribeiro, CG, Lopes dos Santos, A, Trefault, N, Marie, D, Lovejoy, C, Vaulot, D. 2024. Arctic phytoplankton microdiversity across the marginal ice zone: Subspecies vulnerability to sea-ice loss. *Elementa: Science of the Anthropocene* 12(1). DOI: <https://doi.org/10.1525/elementa.2023.00109>

Domain Editor-in-Chief: Jody W. Deming, University of Washington, Seattle, WA, USA

Associate Editor: Kevin R. Arrigo, Department of Earth System Science, Stanford University, Stanford, CA, USA

Knowledge Domain: Ocean Science

Published: May 13, 2024 **Accepted:** March 03, 2024 **Submitted:** August 05, 2023

Copyright: © 2024 The Author(s). This is an open-access article distributed under the terms of the Creative Commons Attribution 4.0 International License (CC-BY 4.0), which permits unrestricted use, distribution, and reproduction in any medium, provided the original author and source are credited. See <http://creativecommons.org/licenses/by/4.0/>.



Elem Sci Anth is a peer-reviewed open access journal published by University of California Press.

OPEN ACCESS 